AN INVESTIGATION ON DIMENSIONAL ACCURACY OF FUSED DEPOSITION MODELING (FDM) PROCESSED PARTS USING FUZZY LOGIC

A THESIS SUBMITTED IN PARTIAL FULFILLMENT OF THE REQUIREMENTS FOR THE DEGREE OF

MASTER OF TECHNOLOGY
IN
MECHANICAL ENGINEERING

[Specialization: Production Engineering]

By

RANJEET KUMAR SAHU

209ME2205

Under the supervision of

Prof. S.S.MAHAPATRA

DEPARTMENT OF MECHANICAL ENGINEERING
NATIONAL INSTITUTE OF TECHNOLOGY ROURKELA
ORISSA (INDIA)

Dedicated to my parents

———————— * ————————

NATIONAL INSTITUTE OF TECHNOLOGY ROURKELA

CERTIFICATE

This is to certify that thesis entitled, **"AN INVESTIGATION ON DIMENSIONAL ACCURACY OF FUSED DEPOSITION MODELING (FDM) PROCESSED PARTS USING FUZZY LOGIC"** submitted by **RANJEET KUMAR SAHU** in partial fulfillment of the requirements for the award of **Master of Technology** Degree in ***Mechanical Engineering*** with "**Production Engineering**" specialization during session 2010-2011 in the Department of Mechanical Engineering, National Institute of Technology, Rourkela.

It is an authentic work carried out by him under my supervision and guidance. To the best of my knowledge, the matter embodied in this thesis has not been submitted to any other university/ institute for award of any Degree or Diploma.

Date:

(Dr. S.S.MAHAPATRA)
Dept. of Mechanical Engineering
National Institute of Technology,
Rourkela-769008

ACKNOWLEDGEMENT

Successful completion of work will never be one man's task. It requires hard work in right direction. There are many who have helped to make my experience as a student a rewarding one. In particular, I express my gratitude and deep regards to my thesis supervisor **Dr. S.S. Mahapatra, Professor, Department of Mechanical Engineering, NIT Rourkela** for kindly providing me to work under his supervision and guidance. I extend my deep sense of indebtedness and gratitude to him first for his valuable guidance, inspiring discussions, constant encouragement & kind co-operation throughout period of work which has been instrumental in the success of thesis.

I extend my thanks to **Dr. R.K. Sahoo, Professor and Head, Dept. of Mechanical Engineering** for extending all possible help in carrying out the dissertation work directly or indirectly.

I express my sincere gratitude to **A.K. Sood, Assistant Professor, Department of Manufacturing Engineering, NIFFT, Ranchi** and other staff members for their indebted help in carrying out experimental work and valuable suggestions. I am also thankful to all the staff members of the department of Mechanical Engineering, NIT Rourkela and to all my well wishers for their inspiration and help.

I greatly appreciate & convey my heartfelt thanks to my friends A.Mondal, A.Mehar, G.Beriha, A.Srivastav, dear ones & all those who helped me in completion of this work.

I feel pleased and privileged to fulfill my parent's ambition and I am greatly indebted to them for bearing the inconvenience during my M Tech. course.

RANJEET KUMAR SAHU

ABSTRACT

Fused deposition modeling (FDM) is an additive manufacturing technology for rapid prototyping that can build 3D complex geometry parts in least possible time with minimum human intervention and without use of tooling. The process parameters such as layer thickness, orientation, raster angle, raster width and air gap along with their interactions largely influence on dimensional accuracy of FDM processed ABSP 400 (Acrylonitrile-butadine-styrene) part which can be expressed as change in length, width and thickness. This study presents experimental data and fuzzy decision making logic in integration with the Taguchi method for improving the dimensional accuracy of FDM built parts. It is observed that length and width decreases but thickness shows positive deviation from desired value of the built part. Optimum parameters setting to minimize change in length, width and thickness of standard test specimen have been found out using Taguchi's parameter design. Experimental results indicate that optimal factor settings for each response are different. Therefore, all the three responses are expressed in a single response index through fuzzy logic approach. The process parameters are optimized with consideration of all the performance characteristics simultaneously. An inference engine is developed to perform the inference operations on the rules for fuzzy logic based on Mamdani method. This study also presents two prediction models- one based on Taguchi approach and the other on ANN approach for assessment of dimensional accuracy of FDM built parts subjected to different operating conditions. The predicted values obtained from Taguchi's additive model and ANN model are in good agreement with the values from the experimental data with mean absolute percentage error of 3.16 and 0.15 respectively. It was found that ANN model is able to predict overall performance characteristic at all operating condition to a higher degree of accuracy. Finally, experimental results are provided to confirm the effectiveness of the proposed fuzzy approach.

Contents

LIST OF FIGURES

List of Tables

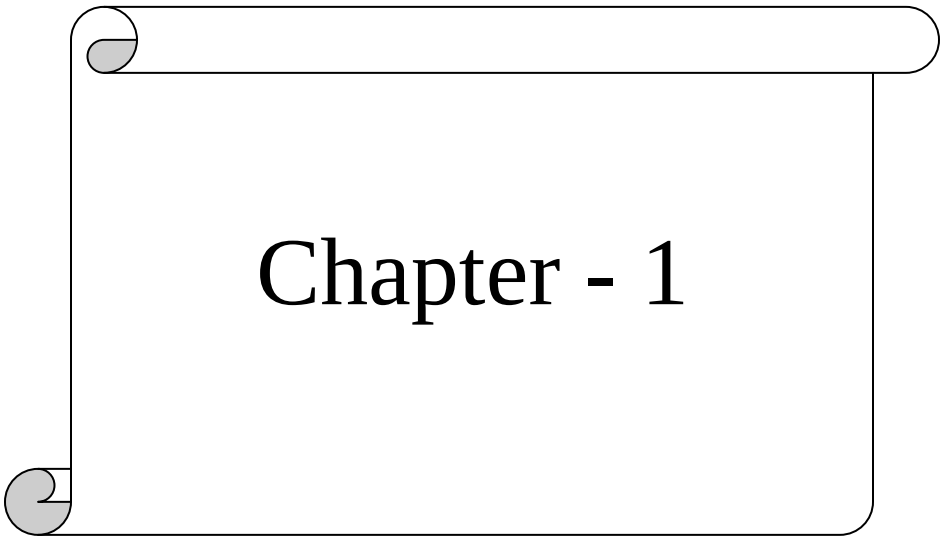
Chapter - 1

Chapter 1

INTRODUCTION

To remain competitive in the market, reduction in product development time became a major concern for industries and hence, industries are looking forward to shift their focus from traditional product development methodology to rapid fabrication techniques [1]. Besides, to obtain prototype parts quickly being able to test for component fit and function can help industries to market the product faster than their competitors. A wide variety of parts building methods have been developed but most of these methods require a long process cycle, laborious and/or energy intensive. Obviously, new and effective fabrication techniques are highly desirable for prototypes. Application of rapid prototyping (RP) technologies enables one to develop prototype parts quickly to a great extent [2, 3]. Some of the latest developments within the automotive industry have shown how emerging rapid prototyping technologies can be used to reduce the time required for designing and manufacturing of prototypes. Rapid prototyping refers to a number of automated machines or manufacturing methods like stereo lithography (SL), fused deposition modeling (FDM), selective laser-sintering (SLS), and laminated object manufacturing (LOM) which rapidly fabricate three dimensional (3D) solid models from CAD data automatically without application of tooling and least human intervention with reasonable time and cost [4, 5]. Another advantage with RP is to produce functional assemblies by merging sub-assemblies into single unit at the computer aided design (CAD) stage and thus reduces part counts, handling time, and storage requirement and avoids mating and fit problem [6, 7]. In general, rapid prototyping method begins with creating a CAD file or solid modeling file (in STL file format) to represent the object geometry as shown in Figure 1.1, slicing this file into a multiple-layer data format representing the horizontal cross sections of the part as shown in Figure 1.2 and converting this layer-wise data into proper numerical codes. These codes are then used to control the X–Y–Z movements of a material-depositing nozzle and an object-supporting platform [8]. A plastic filament or metal wire is unwound from a coil and supplies material to an extrusion nozzle. The nozzle is heated to melt and extrude out small beads of thermoplastic material. Then corresponding to the virtual cross section from the CAD model, each layer is built

on the preceding layer by each machine's particular material fabrication technology and are joined automatically to create the final model or part [9].

Figure 1.1: CAD file representing a model

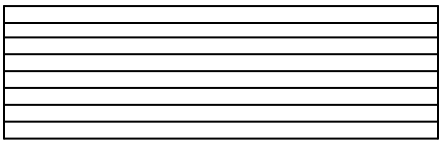

Figure 1.2: Slicing CAD file representing horizontal cross section of model

In this study, the RP technique uses fused deposition modeling (FDM) as an additive manufacturing technology to fabricate 3D parts. Fused deposition modeling is commonly used for modeling, prototyping and production applications. Fused deposition modeling first introduced in the late 1980s, was developed to produce high quality 3D built parts with complex geometries [10]. FDM works on the principle of laying down materials in layers.

Today, the fused deposition modeling processed parts are widely used in automobiles, medical fields, aerospace industries, household equipments, computers, construction of machines, etc. Although RP is an efficient technology for reduction in intricate parts build time and production of parts without use of tools but its full scale application has not gained much emphasis because influence of various process parameters on dimensional accuracy, part strength, build time and surface quality of built parts have not been adequately addressed [11, 12, 13, 14]. Hence, it is absolutely necessary to understand the shortcomings of a process before recommending for industrial application. It has been proposed that improvement of surface quality, part strength, build time, accuracy and repeatability are key issues to be addressed for successful implementation of RP technology [13, 14]. A good number of researchers have suggested that by adjusting the process parameters suitably during fabrication stage part accuracy, strength and quality may be improved [15]. For achieving better dimensional accuracy of FDM built parts, it is important to select process parameters and study the effect of these parameters on responses. Usually, the desired fused deposition modeling process parameters are determined based on experience or referring to machine manual/handbook. However, this does not ensure that the selected process parameters result in optimal or near optimal response for that

particular FDM machine and environment. Therefore, an alternative approach based on the Taguchi method is used in this study as an efficient method to determine the optimal process parameters. This method provides a simple and systematic approach to optimizing designs for performance, quality and cost [16, 17]. Parameter design, based on the Taguchi method, can optimize the performance characteristic through the setting of process parameters and can reduce the sensitivity of the system performance to sources of variation. Taguchi method can understand the process parameters and their possible interaction effects on responses like accuracy of dimensions in different directions of fused deposition modeling built parts with minimum experimental runs [18] and propose an additive (predictive) equation. However, most published Taguchi applications to date have been concerned with the optimization of a single performance characteristic. When multiple performance characteristics are considered, the Taguchi approach becomes unsuitable because several problems are encountered in the optimization of a process with multiple responses. For example, the category of each performance characteristic may not be same and the importance of the performance characteristics may differ [19, 20]. Therefore, in this study, the use of fuzzy decision-making logic to perform fuzzy reasoning of multiple performance characteristics has been used. It is shown that optimization of multiple performance characteristics can be transformed into optimization of a single performance index through fuzzy logic. As a result, the integration of fuzzy logic with the Taguchi method can be used to solve optimization of the multiple performance characteristics. Here, optimization of multi-output performance measures such as change in length, width and thickness of FDM built parts is studied using the proposed approach. All the responses need to be individually minimized whereas overall multi-response performance index, the multiperformance characteristic, is maximized.

Like any experimental investigation, dimensional accuracy trials on FDM built parts also demand substantial amount of time, energy and materials. Hence, to supplement to the experiments artificial neural network is adopted. Over the last two decades, different modeling methods based on artificial neural networks (ANNs) have been used by many researchers for a variety of engineering applications. ANNs are a family of massively parallel architectures that solve difficult problems via the cooperation of highly interconnected but simple computing elements (or artificial neurons) arranged in layers. ANN represents a powerful tool for the

identification of the relevant parameters and their interactions especially when relationships are very complex and highly non-linear. In the present study, predictive model based on artificial neural network have been presented for assessment of dimensional accuracy of FDM built parts subjected to different operating conditions. Taguchi's orthogonal array (OA) used for experimental data collection in a systematic fashion helps to develop valid ANN predictive model conveniently. The model is expected to perform better compared to additive model generated in Taguchi method because non-linearity is not considered in Taguchi's predictive model. Finally, a comparative study of effectiveness of both the models has been made.

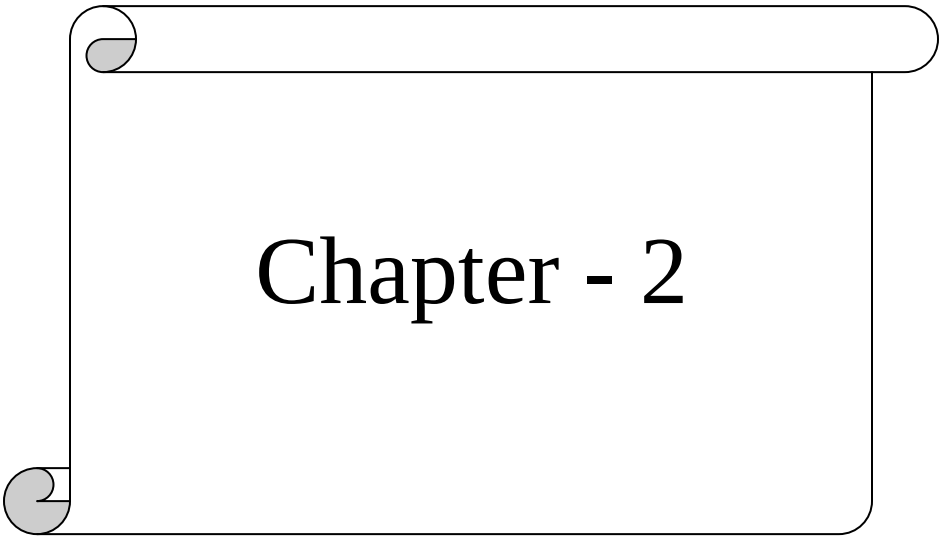
Chapter - 2

Chapter 2

LITERATURE REVIEW

A study made by Vasudevarao et al. [21] shows that when parts are fabricated using ABS 400 plastic on a FDM 1650 machine, layer thickness and part orientation significantly affect surface roughness. Es Said et al. [22] have observed that raster angle causes anisotropic behavior of FDM built parts and orientation influences alignment of polymer molecules along the direction of deposition during fabrication. Since semi-molten filament is extruded from nozzle tip and solidified in a chamber maintained at certain temperature, change of phase is likely to occur. As a result, volumetric shrinkage takes place resulting in weak interlayer bonding and high porosity. Khan et al. [23] have identified important parameters and their levels for improving the flexibility of FDM built parts using design of experiments approach. They have concluded that layer thickness, raster angle and air gap influence the elastic performance of the FDM ABS prototype. Studies have demonstrated that compressive strength is severely affected by build direction in RP systems [24]. Anitha et al. [25] uses Taguchi method to determine the effect of layer thickness, raster width and deposition speed each at three levels on the surface roughness of FDM part. The results indicate that layer thickness is the most influencing process parameter affecting surface roughness followed by raster width and deposition speed. Several attempts have been made to improve the part accuracy, surface finish, strength, etc. by proper adjustment of process parameters by numerous researchers. Lee et al. [24] have performed experiments on cylindrical parts made using three RP processes FDM, 3D printer and nano-composite deposition (NCDS) to study the effect of build direction on compressive strength. Experimental results show that, out of three rapid prototyping technologies, parts build by NCDS are highly affected by the build direction. When material is extruded from nozzle, it cools from glass transition temperature to chamber temperature causing inner stresses to be developed due to uneven deposition speed resulting in inter layer and intra layer deformation that appear in the form of cracking, de-lamination or even part fabrication failure. These phenomena combine to affect the part strength and dimension [26]. It has been observed that deformation is more in

bottom layers than upper layers. Higher the stacking section lengths, deformation becomes larger. If chamber temperature increases, deformation will gradually decrease and become zero when chamber temperature equals glass transition temperature of material. Therefore, it is proposed that material used for part fabrication must have lower glass transition temperature and linear shrinkage rate. Also the extruded fibre length must be small.

Simulation of FDM process using finite element analysis (FEA) shows that distortion of parts is mainly caused due to accumulation of residual stresses at the bottom surface of the part during fabrication [27]. Pandey and Ragunath [28] have shown that laser power and scan length are most influencing process variables along X direction, laser power and beam speed are significant along Y direction and beam speed, hatch spacing and part build temperature are significant along Z direction while studying shrinkage phenomena in Selective Laser Sintering part. Zhou et al. [29] studied the effect of five control factors such as layer thickness, overcure, hatch spacing, blade gap, and part location on build platform and few selected interactions on the accuracy of SLS parts. It has been observed that the factor settings for maximum accuracy depend on geometrical features in the part. Campanelli et al. [30] have recommended that hatch overcure and border overcure must be set at their maximum level for improving part accuracy when layer thickness is high. If low layer thickness is desired then hatch overcure should be maintained at medium level and border overcure at maximum level. These process settings not only improve part accuracy but also eliminate the necessity for post curing the SLS parts. Ahn et al. [31] have pointed out that process parameters such as air gap and raster orientation significantly affect the FDM processed part strength as compared to other parameters like raster width, model temperature and color through experimental design and analysis. Venkata et al. [32], Byun and Lee [33] have pointed out that orientation is an important process parameter for part strength, dimensional accuracy, surface finish, part build time and cost in layered manufacturing. Sood et al. [18] have empirically shows that mechanical properties like tensile strength and flexural strength uniformly decreases with increase in orientation angle. The major reasons for decrease in mechanical properties may be caused due to void formation and thermally induced stresses in FDM built parts. Such detrimental effects may be reduced by proper adjustment of part orientation along with other process parameters. Bellehumeur et al. [34] have experimentally demonstrated that bond quality between adjacent filaments depends on

envelope temperature and variations in the convective conditions within the building part while testing FDM specimen strength. Temperature profiles reveal that temperature at bottom layers rises above the glass transition temperature and rapidly decreases in the direction of movement of extrusion head. The minimum temperature increases with the number of layers. Microphotographs indicate that diffusion phenomenon is more prominent for adjacent filaments in bottom layers as compared to upper layers. Literature unveil that quality of built parts can be significantly enhanced without incurring any additional cost in hardware and software if process parameters are properly adjusted during fabrication stage [35, 15]. The foregoing discussions reveal that properties of FDM processed parts are sensitive to processing parameters because parameters affect meso-structure. Also non-uniform heating and cooling cycles due to inherent nature of FDM build methodology results in stress accumulation in the built part resulting in the distortion and dimensional inaccuracy which are primarily responsible for weak bonding [26].

Based on literature study, it has been found that the effect of process parameters in improving quality of FDM built parts, specifically, dimensional accuracy have been devoted to a limited extent. Since dimensional accuracy is important for component fit and function, therefore it is absolutely essential to establish best parameter settings through a structured methodology for obtaining the better dimensional accuracy of FDM processed part.

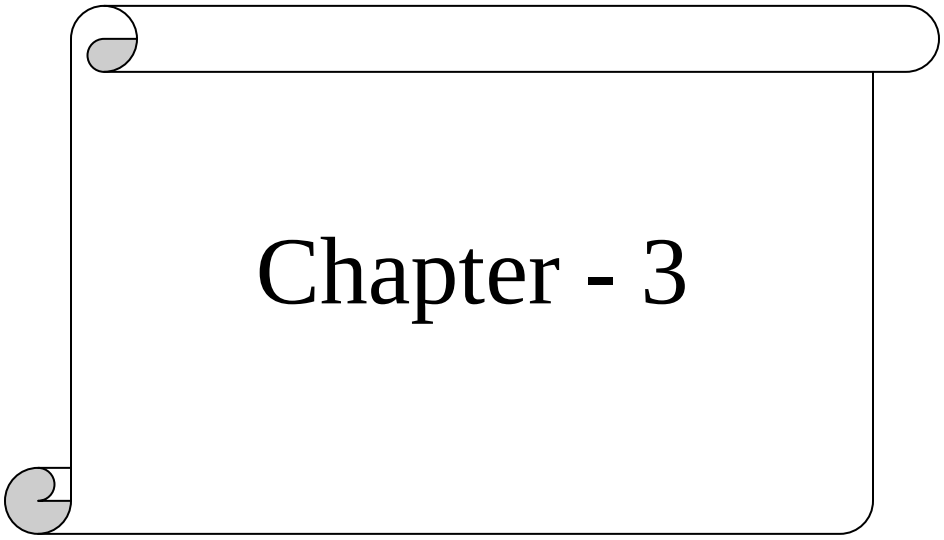
Chapter - 3

Chapter 3

EXPERIMENTAL DETAILS

Fused deposition modeling (FDM) is one of the rapid prototyping processes that build part of any geometry by sequential deposition of material on a layer by layer basis. Existing examples tend to prove that this process offer time and cost advantages over conventional technologies [3, 36]. One of the current challenges faced by FDM users is the quality of parts produced, which is allied with the accurate application of the specified performance [37]. This makes it essential to understand the performance of FDM process parts with the variation of process parameters so as to make them reliable for industrial applications. In this study, dimensional accuracy is considered as measure of part quality in accordance to industrial requirements. To achieve this, the present chapter describes the materials used for FDM part fabrication and also presents the details of the part fabrication methodology related to design of experiment technique based on Taguchi method.

3.1 Material

The material used for test specimen fabrication is acrylonitrile butadiene styrene (ABS P400). ABS (chemical formula $((C_8H_8 \cdot C_4H_6 \cdot C_3H_3N)_n)$ is a common thermoplastic. ABS is derived from acrylonitrile, butadiene, and styrene and carbon as shown in Figure 3.1. It contains 90-100% acrylonitrile/butadiene/styrene resin and may also contain mineral oil (0-2%), tallow (0-2%) and wax (0-2%). Acrylonitrile is a synthetic monomer produced from propylene and ammonia; butadiene is a petroleum hydrocarbon obtained from the C_4 fraction of steam cracking; styrene monomer is made by dehydrogenation of ethyl benzene - a hydrocarbon obtained in the reaction of ethylene and benzene. ABS is a co-polymer made by polymerizing styrene and acrylonitrile in the presence of poly-butadiene. The result is a long chain of poly-butadiene criss-crossed with shorter chains of poly (styrene-co-acrylonitrile). The nitrile groups from neighbouring chains, being polar, attract each other and bind the chains together, making ABS stronger than pure polystyrene.

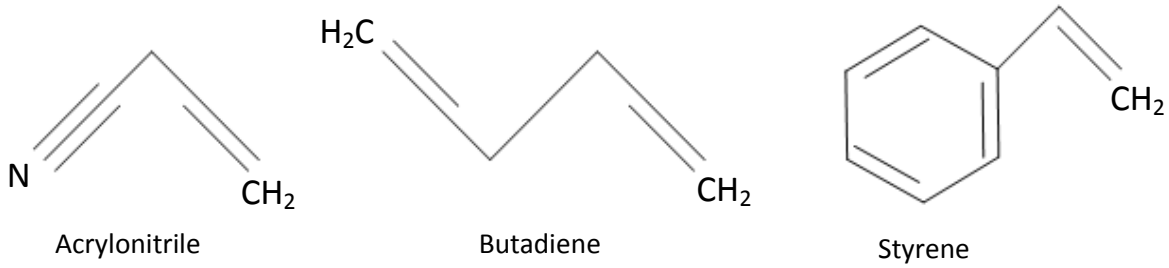

Figure 3.1: Monomers in ABS polymer

Its three structural units provide a balance of properties with the acrylonitrile providing heat resistance, butadiene imparting good impact strength and the styrene gives the copolymer its rigidity. The most significant advantages of ABS plastic are high hardness and impact strength, high toughness, high chemical and thermal resistance, resistance to distortion from humidity, negligible creep and easy processing while a relatively low fatigue strength is a disadvantage [38, 39].

3.2 Experimental design

In conventional experiments, effect of only one factor is investigated independently at a time keeping all other factors at fixed levels. Therefore, visualization of impact of various factors in an interacting environment really becomes difficult. Thus, more experimental runs are required for the precision in effect estimation, general conclusions cannot be drawn and the optimal factor settings are difficult to obtain. To overcome this problem, design of experiment (DOE) approach is used to effectively plan and perform experiments, using statistics and is commonly used to improve the quality of products or processes. Design of experiments is a robust analysis tool for modeling and analyzing the influence of control factors on performance output. FDM is such a process in which a number of control factors collectively determine the performance output in other words the part quality. Hence, in the present work Taguchi's parameter design can be adopted to optimize the process parameters leading to the improvement in dimensional accuracy of the part and study the effect of various parameters including their possible interactions. The most important stage in the DOE lies in the selection of the control parameters and their levels. Therefore, a large number of parameters are initially included so that

insignificant process variables can be identified at earliest opportunity. FDM process has large number of process related parameters which are briefly defined as follows [32, 33, 40]:

- ❖ Part fill style

  Determines the fill pattern used to build a solid model. It is of two types:

  - Perimeter/rasters: Creates a part fill consisting of a single outer contour and internal raster fill.
  - Contours to depth: Fills the part with an outer contour, internal contours and internal raster fills. The number of additional contours is determined by the depth of contours value.

- ❖ Contour width

  The width of the contour tool path that surrounds each of the part curves. Every part curve is filled by using at least one contour.

- ❖ Part interior style

  Choose the manner in which part interior is filled. It is of three types:

  - Solid normal: Fills the part completely.
  - Sparse: Minimize the amount of material use. Utilizes a unidirectional raster
  - Sparse double dense: Minimizes the amount of model material used, but utilizes a cross hatch raster pattern (instead of unidirectional) for added strength.

- ❖ Visible surface

  The intent of this feature is to maintain part appearance while allowing for a coarser, faster fill. The default choice is Normal rasters.

- ❖ Part XY shrinkage factor

  The shrinkage factor applied in the XY plane.

- ❖ Part Z shrinkage factor — The shrinkage factor applied in the Z direction.
- ❖ Perimeters to raster air gap — The gap between the innermost contour and the edge of the raster fill inside of the contour.
- ❖ Layer thickness — It is a thickness of layer deposited by nozzle and depends upon the type of nozzle used.
- ❖ Orientation — Part build orientation or orientation refers to the inclination of part in a build platform with respect to X, Y, Z axis where X and Y-axis are considered parallel to build platform and Z-axis is along the direction of part build.
- ❖ Raster angle — It is the direction of raster relative to the X-axis of build table.
- ❖ Part raster width (raster width) — Width of raster pattern used to fill interior regions of part curves.
- ❖ Raster to raster gap (air gap) — It is the gap between two adjacent rasters on same layer.

Previous research suggests that major part of quality output of FDM processed part primarily depends on few control factors [21, 23-25]. Based on these exhaustive literature review, five important control factors such as layer thickness (A), part build orientation (B), raster angle (C), raster width (D) and raster to raster gap (air gap) (E) are considered to study their influence on dimensional accuracy of FDM processed component. The levels of factors are

selected in accordance with the permissible minimum and maximum settings recommended by the equipment manufacturer, experience, and real industrial applications.

The selected control parameters and their values at different levels are listed in Table 3.1 and other parameters (Table 3.1) are kept at their fixed level.

Table 3.1: Parameters and their levels

Fixed Parameters			Control Parameters					
Parameter	Value	Unit	Parameter	Symbol	Level			Unit
					1	2	3	
Part fill style	Perimeter/Raster	–	Layer thickness	A	0.127	0.178	0.254	mm
Contour width	0.4064	mm	Orientation	B	0	15	30	degree
Part interior style	Solid normal	–	Raster angle	C	0	30	60	degree
Visible surface	Normal raster	–	Raster width	D	0.4064	0.4564	0.5064	mm
X Y & Z shrink factor	1.0038	–	Air gap	E	0	0.004	0.008	mm
Perimeter to raster air gap	0.0000	mm						

3.2.1 Taguchi experimental design

Study of five factors at three levels requires 243 (3^5) experiments if classical design of experiment (DOE) is used but same statistically valid results can be obtained if Taguchi method is adopted with lesser number of experiments [41]. In Taguchi design, selection of orthogonal array is an important issue for obtaining valid conclusions and this is used for design of experimental plan and experiments are carried out according to designed plan. To select an appropriate orthogonal array for experiments, the total degrees of freedom must be computed. The degrees of freedom are defined as the number of comparisons between process parameters that must be made to determine which level is better and, specifically, how much better it is. For example, a three level process parameter counts for two degrees of freedom. The degrees of freedom associated with interaction between two process parameters are given by the product of the degrees of freedom for the two process parameters. Here, four interaction effects are

considered as there is more interaction between FDM process parameters during experimentation. Since five factors each at three level and four interactions are considered in this study, the total degree of freedom happens to be 26 (i.e. 10 degrees of freedom owing to five sets of process parameters and 16 degrees of freedom owing to their interactions in FDM process). Once the degrees of freedom are known, next step is to select an orthogonal array to fit the specific task. In this study, the appropriate orthogonal array is L_{27} (3^{13}). This array consists of 13 columns for assigning factors and/or interaction and 27 rows for designating the trial or experimental conditions. To avoid the confounding effect, assignment of factors and interactions is made based on linear graph as shown in Figure 3.2.

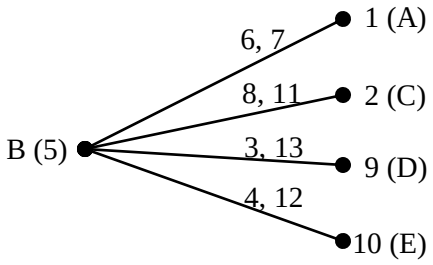

Figure 3.2: Linear graph

Each dot in the linear graph represents the factor with assigned column number in the bracket and line joining two dots corresponds to the interaction between the factors assigned to the column numbers shown on the lines. Out of several parameters, since part orientation seems to influence to a greater extent than any other parameter, therefore, in this study interaction of orientation with all other factors is considered and so it is assigned to column number 5. In order to change the layer thickness, nozzle has to be changed. Frequent change of nozzles is time consuming and involves wastage of material. To prevent this, layer thickness is assigned to column number 1. Factor C is assigned to column 2, factor D is assigned to column 9 and factor E is assigned to column 10 as indicated by linear graph. The experimental layout showing the FDM process parameters and their levels using L_{27} orthogonal array are presented in Table 3.2.

Table 3.2: Experimental layout using an L_{27} orthogonal array

Experiment Number	FDM parameter level				
	Layer thickness (A)	Orientation (B)	Raster angle (C)	Raster width (D)	Air gap (E)
1	1	1	1	1	1
2	1	2	1	2	2
3	1	3	1	3	3
4	1	1	2	2	2
5	1	2	2	3	3
6	1	3	2	1	1
7	1	1	3	3	3
8	1	2	3	1	1
9	1	3	3	2	2
10	2	1	1	2	3
11	2	2	1	3	1
12	2	3	1	1	2
13	2	1	2	3	1
14	2	2	2	1	2
15	2	3	2	2	3
16	2	1	3	1	2
17	2	2	3	2	3
18	2	3	3	3	1
19	3	1	1	3	2
20	3	2	1	1	3
21	3	3	1	2	1
22	3	1	2	1	3
23	3	2	2	2	1
24	3	3	2	3	2
25	3	1	3	2	1
26	3	2	3	3	2
27	3	3	3	1	3

3.3 Specimen fabrication

Specimens are fabricated using FDM Vantage SE machine as shown in Figure 3.3 for dimensional analysis. This machine is developed and marketed by Stratasys Inc., 14950 Martin Drive, Eden Prairie, MN 55334-2020 U.S.A. As compared to other vantage series machines like vantage I, vantage X and vantage S, vantage SE series machine has large build chamber volume (406×355×406mm) as shown in Figure 3.4. It incorporate multiple materials like ABS, ABSi (high impact grade of ABS), Polycarbonate (PC) and PC-ABS and uses water soluble support for

ABS, ABSi and PC-ABS and break away support structure for PC. Support material use can be easily breakaway by hand.

Figure 3.3: FDM Vantage SE machine

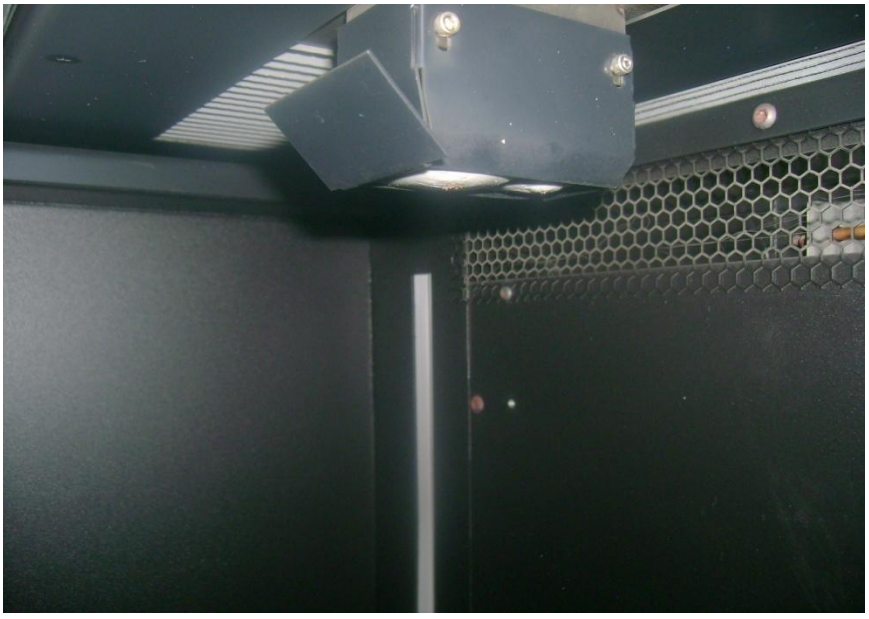

Figure 3.4: Build chamber of vantage SE machine

It has two auto load model material and two auto load support material canisters with 1510 cm^3 modeling material per canister as shown in Figure 3.5. Vantage SE machine has automatic changeover facility between canisters [40].

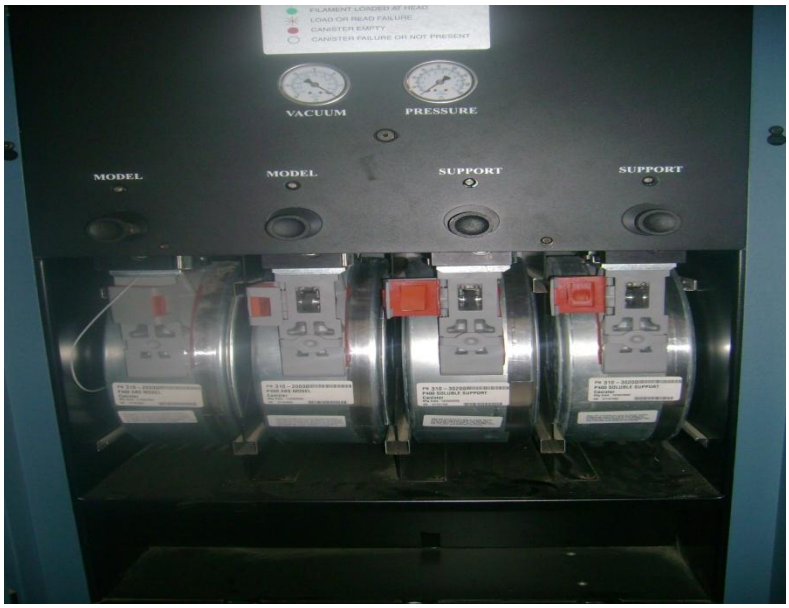

Figure 3.5: Loaded model and support material canisters

3D solid model of test part as shown in Figure 3.6 is generated using CATIA V5 software and exported as STL (stereolithography) file. STL file is imported to FDM software (Insight). Software breaks the STL model into individual slices and generate tool path.

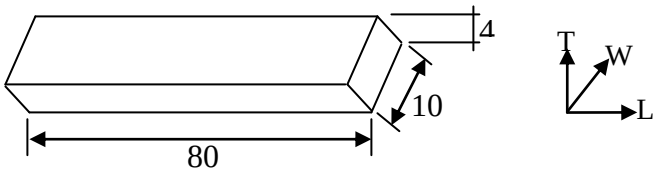

Figure 3.6: Test specimen for dimensional analysis (dimensions are in mm)

L, W and T denote direction in length, width and thickness

Here, control parameters (Table 3.1) are set as per experiment layout (Table 3.2) and other parameters (Table 3.1) are kept at fixed level. The ABS thermoplastic material used in FDM process will melt at a preselected temperature and rapidly solidify upon adhering to the previous

layer. The build ABS P400 material in the form of a filament (flexible strand) is supplied from a supply source spool to the head of the machine as shown in Figure 3.7. The filament of a solid material is introduced into a channel of the nozzle. FDM use two nozzles, one for part (model) material deposition and other for support material deposition, both works alternatively (Figure 3.7).

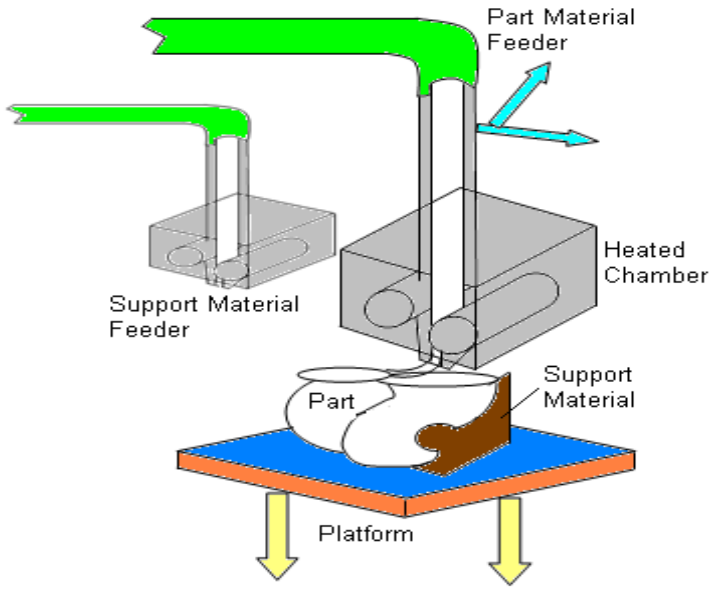

Figure 3.7: Schematic representation of FDM process

One pair of wheels or rollers having a nip in between are utilized as material advance mechanism to grip a filament of modeling material and advance it into a heated chamber or liquefier head as shown in Figure 3.8. The front end, near a nozzle tip the material is heated above its solidification temperature by a heater (liquefier) and extruded out in a semi-molten state. The first layer of a solidifying material dispensed from the nozzle is deposited on to a surface of the platform and upon completion of the first layer, a second layer of material is then deposited onto the first layer and adhered thereto as shown in Figure 3.9. These procedures are repeated until the 3-D physical model is obtained [4, 42]. The nozzle is moved relative to the platform on an X-Y plane and build platform moves along the Z-direction. The drive motions are provided through drive signals input to the drive motors from CAD/CAM system.

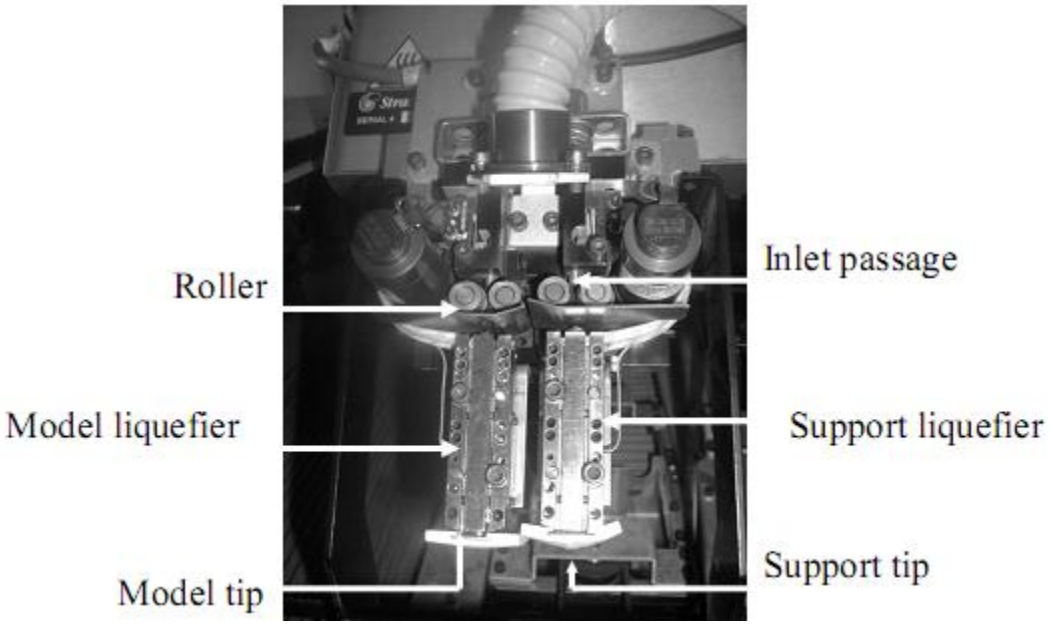

Figure 3.8: Head assembly

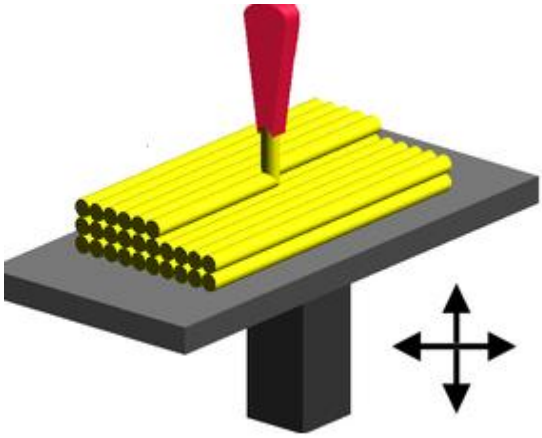

Figure 3.9: Molten material laying down in layers

3.4 Measurement of dimensional accuracy

Three parts per experiment are fabricated as shown in Figure 3.10 using FDM Vantage SE machine. Three readings of length, width and thickness are taken per sample and mean is taken as representative value for each of these dimensions. Dimensions are measured using Mitutoyo vernier calliper having least count of 0.01 mm. Measured values show that there is

shrinkage in length (L) and width (W) but thickness (T) is always more than the CAD model value.

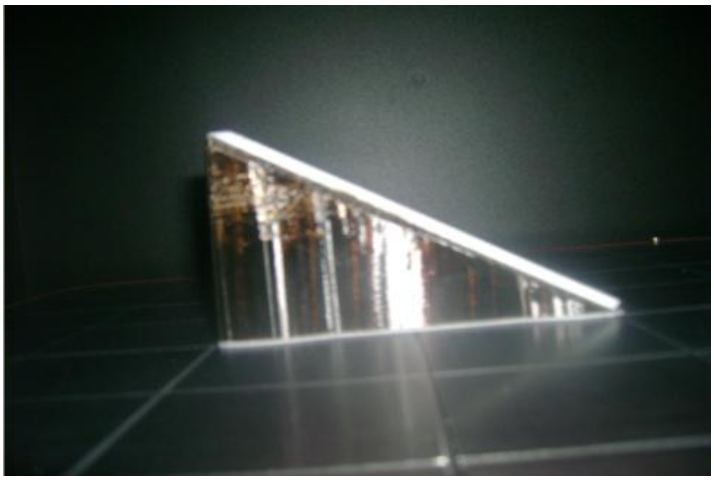

Figure 3.10: FDM built part

Change in dimension is calculated using Eq. (1).

$$\Delta X = \left| X - X_{CAD} \right| \quad (1)$$

where X is the measured value of length or width or thickness, X_{CAD} represent the respective CAD model value and ΔX represent change in X. The experimental observed data for responses like change in length (ΔL), width (ΔW) and thickness (ΔT) are presented in Table 3.3.

Table 3.3: Experimental observed data for responses

Experiment Number	Responses		
	ΔL	ΔW	ΔT
1	0.0460	0.0599	0.1166
2	0.0959	0.0433	0.1566
3	0.0853	0.0833	0.1033
4	0.0386	0.0733	0.1066
5	0.1526	0.0499	0.1533
6	0.1413	0.0433	0.1066
7	0.0226	0.0533	0.1266
8	0.1100	0.0666	0.1600
9	0.0940	0.0633	0.1499
10	0.0099	0.0200	0.1066
11	0.0266	0.0766	0.1733
12	0.0560	0.0499	0.1800

13	0.0773	0.0366	0.1466
14	0.1126	0.0433	0.1933
15	0.1059	0.0366	0.1800
16	0.0606	0.0366	0.1199
17	0.0733	0.0666	0.1700
18	0.0380	0.0366	0.1466
19	0.0573	0.0199	0.2633
20	0.0506	0.0420	0.3833
21	0.1193	0.0239	0.3766
22	0.0333	0.0180	0.3466
23	0.0286	0.0400	0.4200
24	0.0973	0.0299	0.2566
25	0.0199	0.0280	0.2633
26	0.0486	0.0400	0.3433
27	0.0206	0.0400	0.3066

3.5 Scanning electron microscope

The surfaces of the specimen are examined directly by scanning electron microscope (SEM) JEOL JSM-6480LV as shown in Figure 3.11. The JEOL JSM-6480LV is a high performance, scanning electron microscope with a high resolution of 3.0nm. The low vacuum (LV) mode allows for observation of specimens which cannot be viewed at high vacuum due to excessive water content or due to a non-conductive surface. It can accommodate up to 8 inch dia specimen.

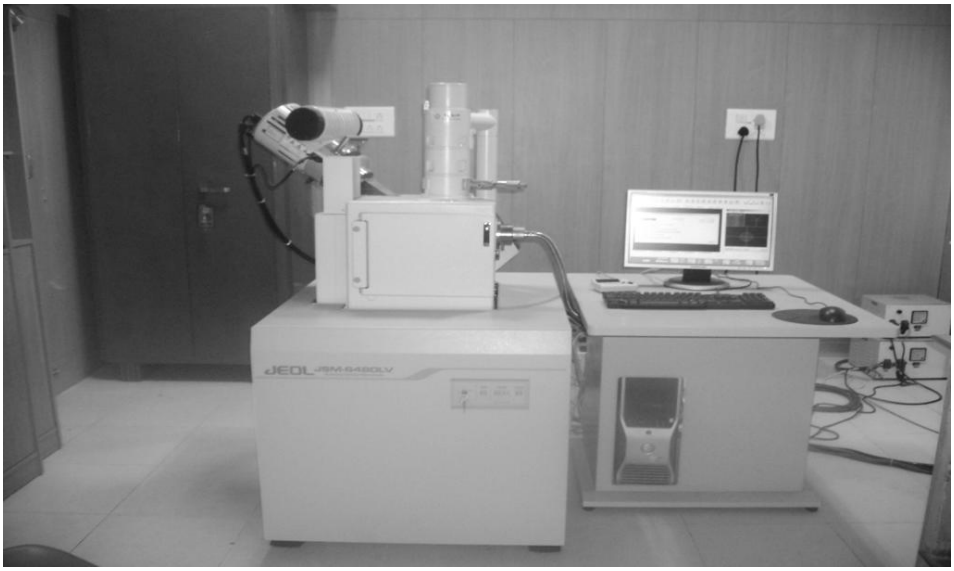

Figure 3.11: Scanning electron microscope (SEM)

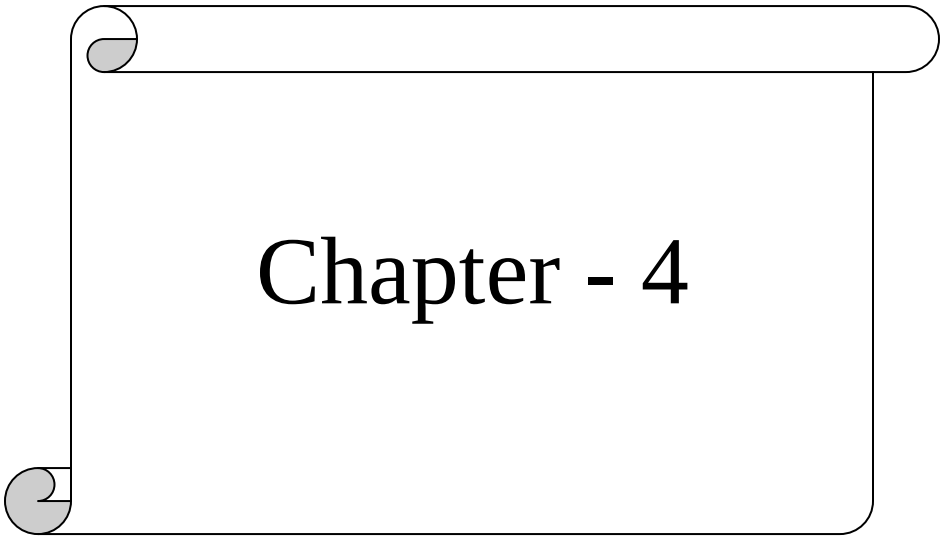
Chapter - 4

Chapter 4

METHODOLOGY

4.1 Signal-to-noise ratio

In the Taguchi method, a loss function is defined to calculate the deviation between the experimental value and the desired value. The signal to noise ratio (S/N) ratio is used to determine the performance characteristics deviating from the desired values. The advantage of using S/N ratio is that it uses a single measure, loss function, which incorporates the effect of changes in mean as well as the variation (standard deviation) with equal priority. Moreover, the results behave linearly when expressed in terms of S/N ratios. The linear behavior of results is an assumption necessary to express performance in the optimum condition. Usually, there are three categories of performance characteristic in the analysis of the signal-to-noise ratio, that is, the lower-the-better, the higher-the-better, and the nominal-the-better. Regardless of the category of the performance characteristics, the larger signal to noise ratio corresponds to the better performance characteristic. Therefore, the optimal level of the process parameters is the level with the highest signal-to-noise ratio. Objective of experimental layout is to reduce the change in length (ΔL), width (ΔW) and thickness (ΔT), respectively. Hence, lower-the-better quality characteristic is considered. The signal-to-noise ratio (η_{ij}) of lower-the-better performance characteristic can be expressed as:

$$\eta_{ij} = -10\log(L_{ij}) \tag{2}$$

$$L_{ij} = \frac{1}{n}\sum_{k=1}^{n} y_{ijk}^{2} \tag{3}$$

where $\boldsymbol{L_{ij}}$ is the loss function of the i th performance characteristic in the j th experiment, n is the number of repetitions and y_{ijk} is the experimental value of the i th performance characteristic in the j th experiment at the k th observation.

4.2 Analysis of variance

Experimental analysis is made using Minitab R14 software. Main effect plot for S/N ratio is used to predict the optimum factor level. Furthermore, a statistical analysis of variance (ANOVA) is performed to identify the process parameters and interactions that significantly affect the performance characteristic. The percentage contribution (%P) of various process parameters and interactions on the selected performance characteristic can be estimated by performing ANOVA test. In addition, significance of factors and interactions can also be determined by comparing calculated F-value with standard F-value at a particular level of confidence (95% in this study). Thus, information about the effect of each controlled parameter on the quality characteristic of interest can be obtained. Calculations needed for ANOVA are shown from Eqs. (4) - (6).

$$SS_A = \left[\sum_{l=1}^{3} \left(\frac{A_l^2}{\eta_{A_l}} \right) \right] - \frac{T^2}{N} \qquad (4)$$

where SS_A is sum of square of factor A, A_l is sum of the observed data associated with l th level of factor A, η_{A_l} is number of observations associated with l th level of factor A, T is sum of all experimental observation and N total number of observations.

Without prejudice to the above general expression (Eq. 4), variation due to the other control factors can also be determined.

$$SS_{A\times B} = \left[\sum_{m=1}^{c} \left(\frac{(A\times B)_m^2}{\eta_{(A\times B)m}} \right) \right] - \frac{T^2}{N} - SS_A - SS_B \qquad (5)$$

where $SS_{A\times B}$ is variation due to the interaction of factors A and B, $(A\times B)_m$ represent sum of data under the mth condition of the combinations of factor A and B, c is number of possible combinations of the interacting factors and $\eta_{(A\times B)m}$ represents number of data points under this condition.

Without prejudice to the above general expression (Eq. 5), variation due to the interaction of other control factors viz., B×C, B×D and B×E can also be determined.

$$SS_T = \sum_{k=1}^{N} y_k^2 - \frac{T^2}{N} \qquad (6)$$

where SS_T is a total sum of square, y_k is experimental value of each observation from k =1 to N. If error degree of freedom becomes zero then factors and interactions having small SS values in comparison to maximum SS present in the ANOVA table are pooled. Once the significant factors and interactions are known, the final step in a design of experiment approach is to predict and verify improvements in performance characteristic values through the use of the combination level of significant control parameters using Taguchi's predictive model.

Three performance measures – change in length,width and thickness are considered with an aim to minimize all these simultaneously at the single factor level setting. However, the Taguchi method is best suitable for optimization of a single performance characteristic whereas fuzzy logic unit combine the entire considered performance characteristic (objectives) into a single value that can be used as the single characteristic in optimization problems. In the present study, to consider the three different responses in the Taguchi method, the S/N ratios corresponding to the ΔL, ΔW and ΔT are processed by the fuzzy logic unit.

4.3 Fuzzy logic unit

This section provides an introduction to fuzzy logic unit. Detailed analysis on fuzzy logic unit can be found in numerous literatures [43, 44, 45, 46]. The structure of the three-input-one-output fuzzy logic unit is shown in Figure 4.1. As outlined in Figure 4.1, a fuzzy logic unit comprises of a fuzzifier, knowledge base (membership functions and fuzzy rule base), an inference engine, and a defuzzifier. These components are described below:

- Fuzzifier: The real input to the fuzzy system is applied to the fuzzzifier. In fuzzy literature, this input is called crisp input since it contains precise information about the specific information about the parameter. The fuzzifier converts this precise quantity to

the form of imprecise quantity like 'small', 'medium', 'large' etc. with a degree of membership to it. Typically, the value ranges from 0 to 1.

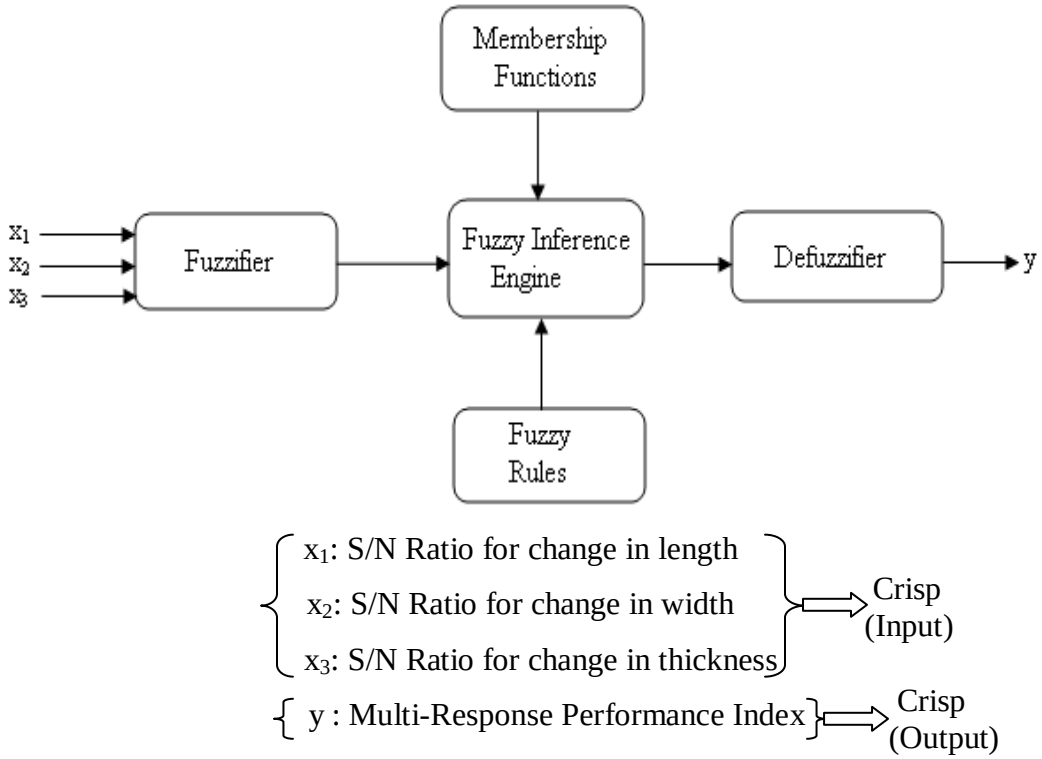

Figure 4.1: Structure of the three-input-one-output fuzzy logic unit

- Knowledge base: The main part of the fuzzy system is the knowledge base in which both rule base and database are jointly referred. The database defines the membership functions of the fuzzy sets used in the fuzzy rules where as the rule base contains a number of fuzzy if-then rules.
- Inference engine: The fuzzy inference engine or inference system or decision-making unit performs the inference operations on the rules. It handles the way in which the rules are combined.
- Defuzzifier: The output generated by the inference block is always fuzzy in nature. A real world system will always require the output of the fuzzy system to the crisp. The job

of the defuzzifier is to receive the fuzzy input and provide real output. In operation, it works opposite to the input block.

In general two most popular fuzzy inference systems are available: Mamdani fuzzy model and Sugeno fuzzy model. The selection depends on the fuzzy reasoning and formulation of fuzzy IF-THEN rules. Mamdani fuzzy model [47] is based on the collections of IF-THEN rules with both fuzzy antecedent and consequent predicts. The benefit of this model is that the rule base is generally provided by an expert and hence to a certain degree it is translucent to explanation and study. Because of its ease, Mamdani model is still most commonly used technique for solving many real world problems.

4.3.1 Development of Mamdani fuzzy model

In the present study, an attempt was made to use fuzzy system (Mamdani model) to estimate the performance index of multiple performance characteristics. With availability of set of measured data input and output of the fuzzy system would be able to evaluate the output for any given input even if a specific input condition had not been covered in the building stage. The proposed Mamdani fuzzy model for evaluation of multiresponse performance index is presented in Figure 4.2. The given model was a multi Input and single output model.

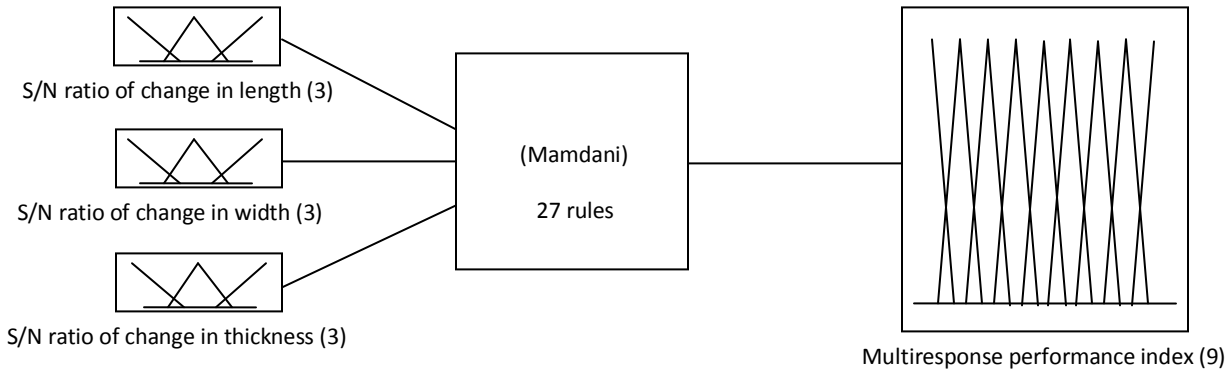

Figure 4.2: Structure of Mamdani fuzzy rule based system for evaluating multiresponse-performance index (MRPI)

The methodology for the development of fuzzy model involved the following steps:

(i) Selection of input and output variables,

(ii) Selection of membership functions for input and output variables,

(iii) Formation of linguistic rule base, and

(iv) Defuzzification.

4.3.1.i Selection of input and output variables

The first step in system modeling was the identification of input and output variables called the system's variables. In this study, the input variables for fuzzy system are S/N ratio of change in length, width and thickness and output variable is multiresponse performance index. The universe of discourse was also decided on the basis of the physical nature of the problem. In the selection procedure, the above mentioned inputs and output were taken in the form of linguistic format which displayed an important role in the application of fuzzy logic.

For example, S/N ratio of change in length = {small, medium, large}, S/N ratio of change in width = {small, medium, large}, S/N ratio of change in thickness = {small, medium, large}. The output variable, multiresponse performance index is divided into = {Tiny, very small, small, small medium, medium, medium large, large, very large, huge}. Linguistic variables are those variables whose values are words in a natural or artificial language and meaning remains same but form varies.

4.3.1.ii Selection of membership functions for input and output variables

Linguistic values were expressed in the form of fuzzy sets. A fuzzy set is usually defined by its membership functions. In general, triangular and trapezoidal membership functions were used to normalize the crisp inputs because of their simplicity and computational efficiency. The triangular membership function as described in Eqs (7) is used to convert the linguistic values in the range of 0 to 1.

$$\text{triangle}\ (x;a,b,c) = \begin{Bmatrix} 0, x \le a \\ \dfrac{x-a}{a-b}, a \le x \le b \\ \dfrac{c-x}{c-b}, b \le x \le b \\ 0, c \le x \end{Bmatrix}$$

or more compactly, by

$$\text{triangle}\ (x;a,b,c) = \max\left(\min\left(\frac{x-a}{b-a},\frac{c-x}{c-b}\right),0\right) \qquad (7)$$

where a,b,c are the parameters of the linguistic value and x is the range of the input variables. In this proposed model, each input have three triangular membership functions, where the output of the proposed model has nine triangular membership functions. The system's input variables as shown in Figure 4.1 are converted to linguistic values depending on grade of membership to the linguistic variable. Similarly, the output, MRPI is divided into nine output zones. The output is expressed in linguistic terms based on grade of membership.

4.3.1.iii Formation of linguistic rule-base

The relationship between input and the output were represented in the form of if-then rules. As per the fuzzy system, the inputs x_1, x_2, x_3 had three membership functions each, hence 27 (3^3) rules can be made. In Mamdani fuzzy model, max-min inference was applied. The rules of the mamdani fuzzy system with three inputs, x_1, x_2, and x_3, and one output y, were generated in the following ways:

Rule 1: if x_1 is A_1, x_2 is B_1 and x_3 is C_1, then y is D_1 else
Rule 2: if x_1 is A_2, x_2 is B_2 and x_3 is C_2, then y is D_2 else
.
Rule n: if x_1 is A_n, x_2 is B_n and x_3 is C_n, then y is D_n.

A_i, B_i, C_i and D_i are the linguistic parameters or membership functions of the inputs (x_1, x_2 & x_3) and output (y). Further, larger the multi-response performance index is, the better the performance characteristic and thus, gives the optimum factor levels.

4.3.1.iv Defuzzification

In this proposed model, a defuzzification method, called the centroid of area (COA) method as expressed in Eq. (8) [48] is adopted to transform the fuzzy inference output into a non-fuzzy value which is known as multiresponse performance index (MRPI).

$$\text{COA}= \frac{\int_y \mu_D(y)\,y\,dy}{\int_y \mu_D(y)\,dy} \qquad (8)$$

where $\mu_D(y)$ is the membership function of the output of fuzzy reasoning, y is output variable (range $\rightarrow$ 0 to 1).

4.4 Neural computation

Fused deposition modeling process involves a large number of conflicting factors and complex phenomena for part build and hardly predict the performance characteristics accurately by mathematical equations. FDM process operating variables influence the responses in a highly non-linear manner. Therefore, artificial neural network (ANN) a robust statistical method, responding to the constraints is implemented in this work to correlate the operating parameters. An artificial neural network is composed of simple elements operating in parallel. These elements are organised into a sequence of layers, each linked by weights. A neural network's structure can be characterized by the connection pattern among elements and the transfer function for transforming input to output in elements. A neural network is trained to perform a particular function by adsjusting the values of the connections (weights) between elements so that a particular input leads to a specific target output as shown in Figure 4.3.

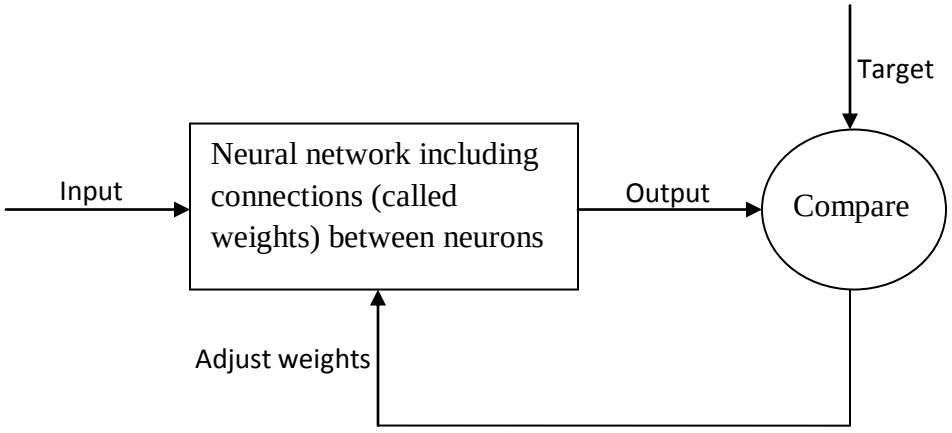

Figure 4.3: Structure of ANN

Here, the network is adjusted based on a comparision of the output and the target, until the network output matches the target.

In ANN approach, a model can be constructed very easily based on the given input and output and trained to predict process dynamics accurately. This technique is especially valuable in processes where a complete understanding of the physical mechanism is very difficult, or even impossible to acquire, as in the case of FDM process. The details of this methodology are described by [49]. In the present analysis factors A, B, C, D and E are taken as five input parameters for training. Each of these parameters is characterized by one neuron and consequently the input layer in the ANN structure have five neurons. The data base is built considering experiments at the limit ranges of each parameter. MRPI values are used to train the ANN in order to understand the input-output correlations. The data is then divided into three categories, namely: (i) a validation category, which is required to define the ANN architectures and adjust the number of neurons for each layer. (ii) a training category, which is exclusively used to adjust the network weights and (iii) a test category, which corresponds to the set that validates the results of the training protocol. The input variables are normalised so as to lie in the same range of 0-1. Different ANN structures (I-H-O) with varying number of neurons in the hidden layer are tested at constant cycles, show and goal (error tolerance). Based on least error criterion, one structure, shown in Table 4.1, is selected for training of the input-output data. Show of 50 is set as training parameter during the training of the input-output data. Number of

Table 4.1: Input parameters selected for training

Input parameters for training	Values
Error tolerance (goal)	0.00001
Show	50
Number of epochs	10,000
Number of neurons in the hidden layer (H)	7
Number of input layer neuron (I)	5
Number of output layer neuron (O)	1

neurons in the hidden layer is varied and in the optimized structure of the network, this number is 7. The number of cycles selected during training is high enough so that the ANN models could be rigorously trained.

A software package MATLAB7.0 R(14) for neural computing using back propagation algorithm is used as the prediction tool for multiresponse performance index under various test conditions. In the present study, backpropagation learning employs a conjugate gradient algorithm [50]. In the conjugate gradient algorithm, a search is performed along conjugate directions which produces generally faster convergence than steepest descent direction. In this algorithm, the length of the weight update (step size) is adjusted at each iteration. A search is made along the conjugate gradient direction to determine the step size which minimizes the performance function along that line. In this study, conjugate gradient Fletcher-Reeves training function (traincgf) is used. The traincgf converges in fewer iterations than gradient descent training function although there is more computation required in each iteration. The three-layer neural network having an input layer (I) with five input nodes, a hidden layer (H) with seven neurons and an output layer (O) with one output node employed for this work is shown in Figure 4.4. Seventy five percent of data is used for training whereas twenty five percent data is used for testing.

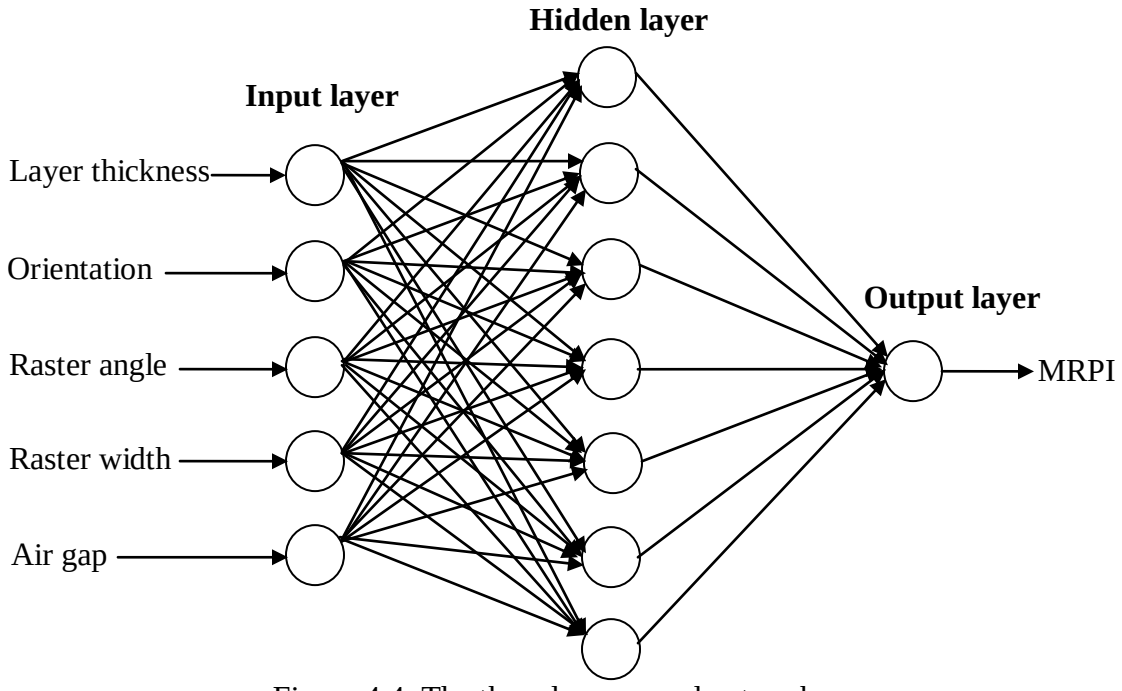

Figure 4.4: The three layer neural network

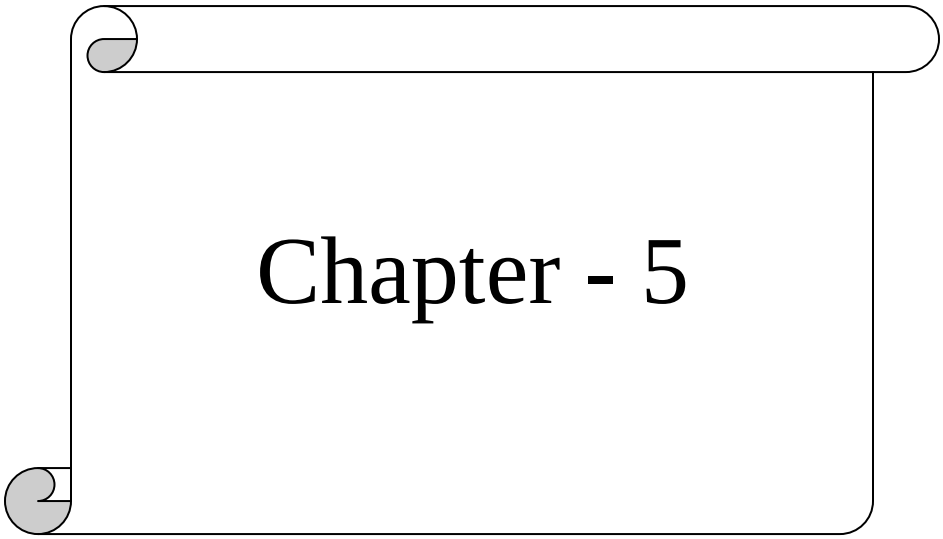
Chapter - 5

Chapter 5

RESULTS AND DISCUSSION

Experimental data on change in dimension (Table 3.3) based on the experimental layout (Table 3.2) is converted to S/N ratio value as shown in Table 5.1 using Eq. (2) for lower the better quality characteristic.

Table 5.1: S/N ratio of experimentally observed ΔL, ΔW and ΔT

Experiment Number	S/N ratio (dB)		
	ΔL	ΔW	ΔT
1	26.7448	24.4515	18.6660
2	20.3636	27.2702	16.1042
3	21.3810	21.5871	19.7180
4	28.2683	22.6979	19.4449
5	16.3289	26.0380	16.2892
6	16.9972	27.2702	19.4449
7	32.9178	25.4655	17.9513
8	19.1721	23.5305	15.9176
9	20.5374	23.9719	16.4840
10	40.0873	33.9794	19.4449
11	31.5024	22.3154	15.2240
12	25.0362	26.0380	14.8945
13	22.2364	28.7304	16.6773
14	18.9692	27.2702	14.2754
15	19.5021	28.7304	14.8945
16	24.3505	28.7304	18.4246
17	22.6979	23.5305	15.3910
18	28.4043	28.7304	16.6773
19	24.8369	34.0229	11.5910
20	25.9170	27.5350	8.3292
21	18.4672	32.4320	8.4824
22	29.5511	34.8945	9.2034
23	30.8727	27.9588	7.5350
24	20.2377	30.4866	11.8149
25	34.0229	31.0568	11.5910
26	26.2673	27.9588	9.2865
27	33.7227	27.9588	10.2686

Main effect plots for S/N ratio of three responses as shown in Figure 5.1 gives the optimum factor levels which are presented in Table 5.5. The significant factors and interactions (Table 5.5) are identified using ANOVA shown in Tables 5.2-5.4 for ΔL, ΔW and ΔT, respectively.

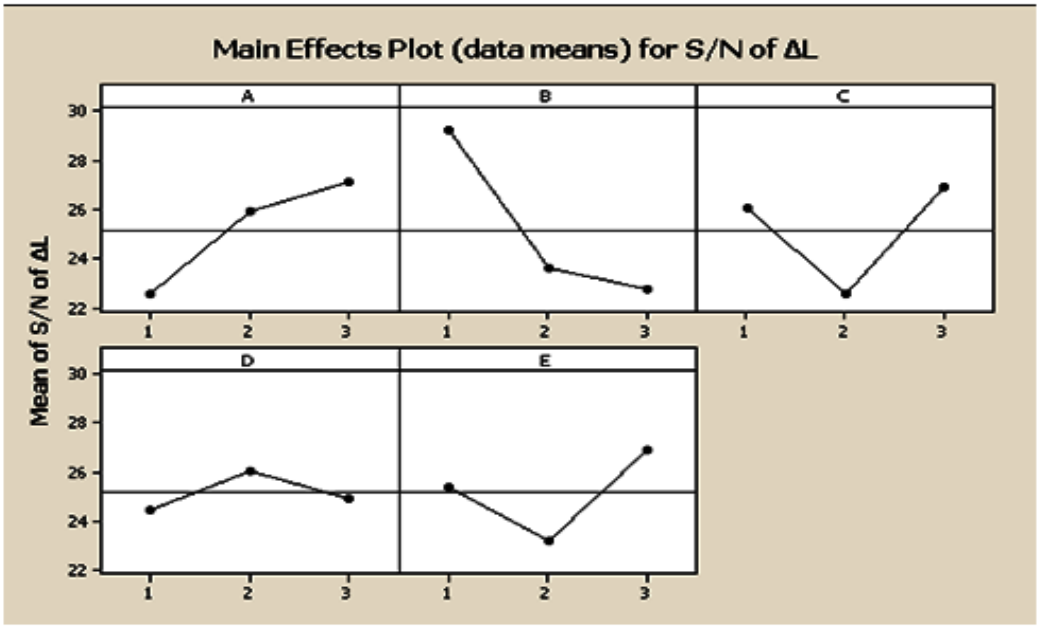

(a)

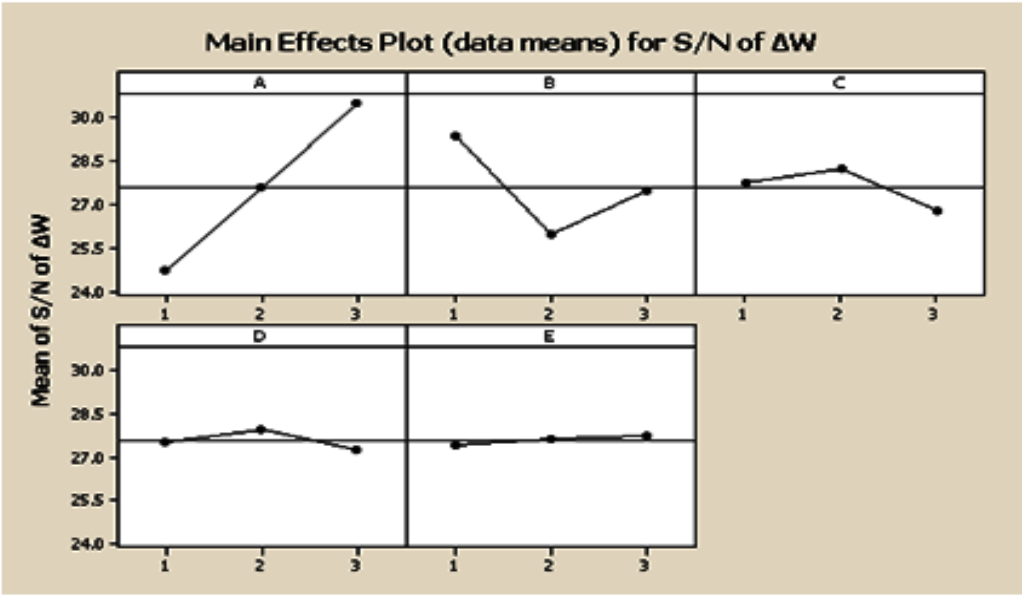

(b)

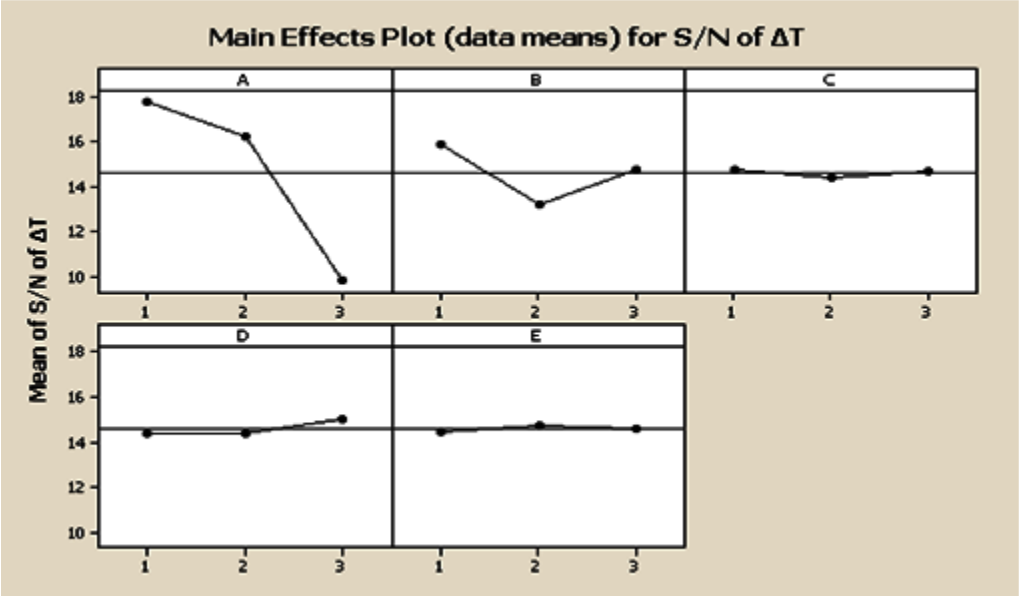

(c)

Figure 5.1: Main effect plot (a) ΔL, (b) ΔW and (c) ΔT for S/N ratio (smaller is better)

Table 5.2: ANOVA for ΔL

Source	DOF	SS	MS	F	%P
A	2	100.892	50.446	2.76	10.67
B	2	226.056	113.028	6.19	23.91
C	2	95.390	47.695	2.61	10.08
D*		12.376	6.188	0.33	1.34
E*		62.016	31.008	1.69	6.55
A×B*		68.116	17.029	0.93	7.20
B×C*		76.581	19.145	1.04	8.10
B×D	4	169.326	42.331	2.32	17.91
B×E	4	134.642	33.660	1.84	14.24
Error	12	219.089	18.257		
Total	26	945.393			100

* Pooled

Table 5.3: ANOVA for ΔW

Source	DOF	SS	MS	F	%P
A	2	150.35	75.175	34.22	44.44
B	2	52.264	26.132	11.89	15.44
C*		9.932	4.966	2.26	2.93
D*		2.248	1.124	0.51	0.66
E*		0.593	0.297	0.14	0.21
A×B	4	53.452	13.363	6.08	15.79
B×C*		15.277	3.819	1.74	4.51
B×D*		2.703	0.676	0.31	0.79
B×E	4	51.534	12.883	5.86	15.23
Error	14	30.753	2.197		
Total	26	338.353			100

* Pooled

Table 5.4: ANOVA for ΔT

Source	DOF	SS	MS	F	%P
A	2	322.682	161.341	169.3	83.17
B	2	34.031	17.016	17.86	8.77
C*		0.529	0.265	0.28	0.18
D*		2.52	1.26	1.32	0.64
E*		0.249	0.125	0.13	0.06
A×B*		5.973	1.493	1.57	1.53
B×C*		5.644	1.411	1.48	1.45
B×D	4	14.091	3.523	3.7	3.63
B×E*		2.246	0.561	0.59	0.57
Error	18	17.161	0.953		
Total	26	387.966			100

*Pooled

Table 5.5: Optimum factor level with significant factors and interactions

Factor	Change in length	Change in width	Change in thickness
A	3	3	1
B	1	1	1
C	3	2	1
D	2	2	3
E	3	3	2
Significant	A, B, C, B×D, B×E	A, B, A×B, B×E	A, B, B×D

From Table 5.5, it has been found that change in length is minimum at A_3 = 0.254mm, $B_1 = 0^0$, $C_3 = 60^0$, D_2 = 0.4564mm and E_3 = 0.008mm, change in width is minimum at A_3 = 0.254mm, $B_1 = 0^0$, $C_2 = 30^0$, D_2 = 0.4564mm and E_3 = 0.008mm and change in thickness is minimum at A_1 = 0.127mm, $B_1 = 0^0$, $C_1 = 0^0$, D_3 = 0.5064mm and E_2 = 0.004mm. Table 7 also shows that A, B, C, B×D, B×E are the significant factors and interactions for affecting change in length; A, B, A×B, B×E for affecting change in width; A, B, B×D for affecting change in thickness.

From Table 5.1, it is observed that shrinkage is predominant in length and width direction but dimension increases from its desired value in thickness direction. Shrinkage along length and width may be attributed to the development of inner stresses resulting from the contraction of depositing fibre. When cooling from extrusion temperature to glass transition temperature, the deposited thermoplastic fibre may be subjected to contraction. However, at this temperature range the deposited fibre can acquire a large deformation with less force and capacity to resist outside force is small. Therefore, in spite of contraction, the inner stresses are not accumulated [31]. But when cooling from glass transition temperature to build chamber temperature, stress (σ) given by Eq. (9) is developed.

$$\sigma = -E\alpha\Delta T \tag{9}$$

where E is Young's modulus of elasticity, α is coefficient of thermal expansion and ΔT is change in temperature. But in FDM, heating and rapid cooling cycles of the material result in non-uniform temperature gradients. This cause stresses to build up leading to distortion, dimensional inaccuracy and inner layer cracking (Figure 5.2) or de-lamination [26]. The reasons for the beneath case are explained as follows:

1. In FDM, heat is dissipated by conduction and forced convection and the reduction in temperature caused by these processes forces the material to quickly solidify onto the surrounding filaments. Bonding between the filaments is caused by local re-melting of previously solidified material and diffusion. This results in uneven heating and cooling of material and develops non-uniform temperature gradients. As a result, uniform stress will not be developed in the deposited material and it may not regain its original dimension completely.

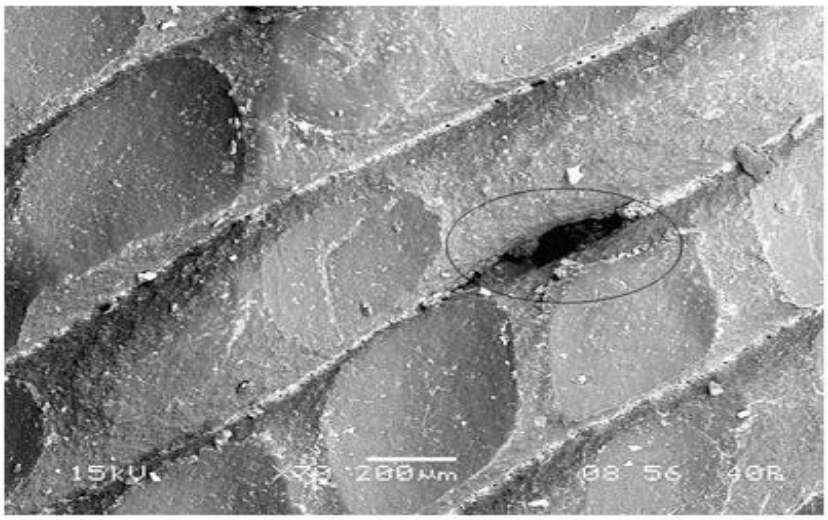

Figure 5.2: SEM image of crack between two rasters

2. Speed at which nozzle is depositing the material may alter the heating and cooling cycle and results in different degree of thermal gradient and thus also affects the part accuracy [27]. At lower slice thickness, nozzle deposition speed is slower as compared to higher slice thickness. Also during deposition, nozzle stops depositing material in random manner (in between depositing a layer and after completely depositing a layer) and return to service location for tip cleaning. While depositing the material at the turns near the boundary of part, nozzle speed has to be decreased and then increase to uniform speed [6]. If deposition path length is small, this will result in non-uniform stress to build up especially near the part boundary.

3. The pattern used to deposit a material in a layer has a significant effect on the resulting stresses and deformation. Higher stresses will be found along the long axis of deposition line. Therefore, short raster length is preferred along the long axis of part to reduce the stresses [51].

4. Stress accumulation also increase with layer thickness and road width [27]. But the thick layer also means fewer layers, which may reduce the number of heating and cooling cycles. Also, a smaller road width will input less heat into the system within the specified period of time but requires more loops to fill a certain area. More loops means more time required for deposition of single layer and more non-uniform nozzle speed. This will keep the deposited material above its desired temperature for regaining its original shape and in the mean time new material will be deposited and contraction of previously deposited material will be constrained.

5. The gap between two rasters in a single layer and voids between rasters of two adjacent layers as shown in Figure 5.3 also effect the heat dissipation and thus may decrease the residual stress.

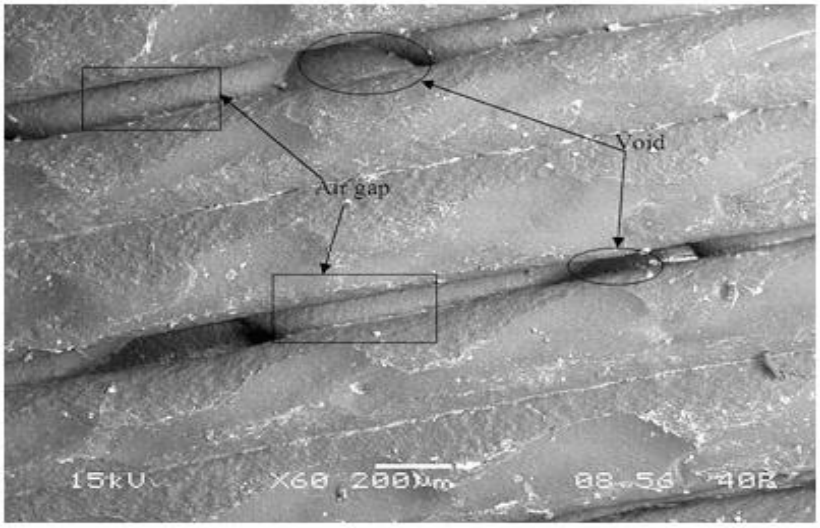

Figure 5.3: SEM image showing air gap

But in case of thickness, it seems that increase is mainly caused due to prevention of shape error and positive slicing method [52, 53]. Consider Figure 5.4, which shows that height of test part (H) is function of its inclination (θ) with respect to build platform, length (L) and thickness (T).

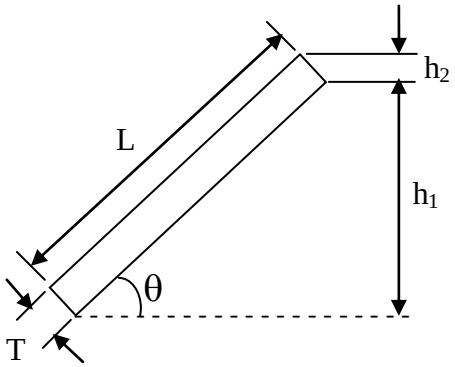

$H = h_1 + h_2$

$h_1 = L \sin\theta$

$h_2 = T \cos\theta$

Figure 5.4: Orientation of part with respect to the base

Height of part consider in this work at maximum orientation of 30^0 will be 43.48 mm. If we slice it with minimum thickness of 0.127 mm, total 342.36 slices will be required by simple arithmetic. Material flow rate is constant, so 0.36 has no meaning and it will be rounded off to

nearest whole number. But to prevent shape error it will round off to one and machine will deposit 343 slices. This argument is true for any orientation of part.

Diffusion of material between neighboring rasters also produces the bump because of overfilling at contact area which results in uneven layer as shown in Figure 5.5. As a result, the next layer which will be deposited on this layer will not get the even planer surface and may result in increase in dimension along the part build direction.

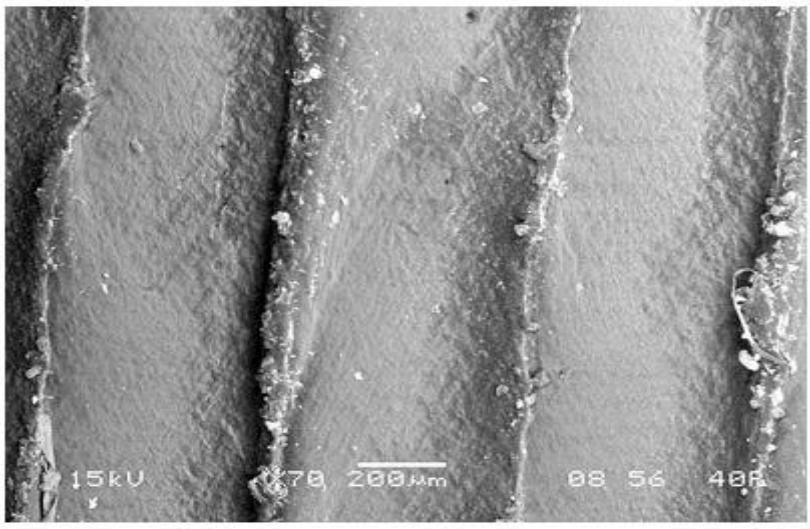

Figure 5.5: SEM image of part showing overfilling at the contact of two raster

These observations show that large number of factors, independently or in combination with each other are influencing the dimensional accuracy of FDM part. From Table 5.5, it is observed that significant factor and interactions are different for different dimensions. Further, optimum factor levels are different in three directions. However, actual fabrication of part is to be done in a manner so that all the dimensions should reach a target value simultaneously, at the common factor level setting. For this, fuzzy decision making logic is used. Fuzzy logic approach has ability to combine all the objectives and transform them into single performance index and give the factor levels which satisfy all the considered objectives simultaneously [54]. In the present study, S/N ratio for ΔL, ΔW and ΔT is taken as system's input linguistic variables and MRPI as output linguistic variable for fuzzy logic approach. Table 5.6 shows the linguistic variables, their linguistic value, and associated fuzzy intervals derived from Table 5.1 and range of output as

mentioned above. From this, graphical representation of input membership functions are shown in Figures 5.6 to 5.8 in which three fuzzy subsets are assigned in the three inputs and output membership functions is shown in Figure 5.9 in which fifteen fuzzy subsets are assigned in the output (Multiresponse performance index). Various degrees of membership of the fuzzy sets are calculated based on the values of x_1, x_2, x_3 and y.

Table 5.6: Inputs and output with their linguistic values and fuzzy intervals

Sl.No.	System's linguistic variable	Variables	Linguistic values	Fuzzy interval
1	Inputs	S/N ratio of change in length	Small	16-26 (dB)
			Medium	18-38 (dB)
			Large	30-40 (dB)
2		S/N ratio of change in width	Small	21-27 (dB)
			Medium	22-34 (dB)
			Large	29-35 (dB)
3		S/N ratio of change in thickness	Small	6-12 (dB)
			Medium	7-19 (dB)
			Large	14-20 (dB)
4	Output	Multiresponse-performance index (MRPI)	Tiny	0-0.1125
			Very small	0.0125-0.2375
			Small	0.1375-0.3625
			Small medium	0.2625-0.4875
			Medium	0.3875-0.6125
			Medium large	0.5125-0.7375
			Large	0.6375-0.8625
			Very large	0.7625-0.9875
			Huge	0.8875-1

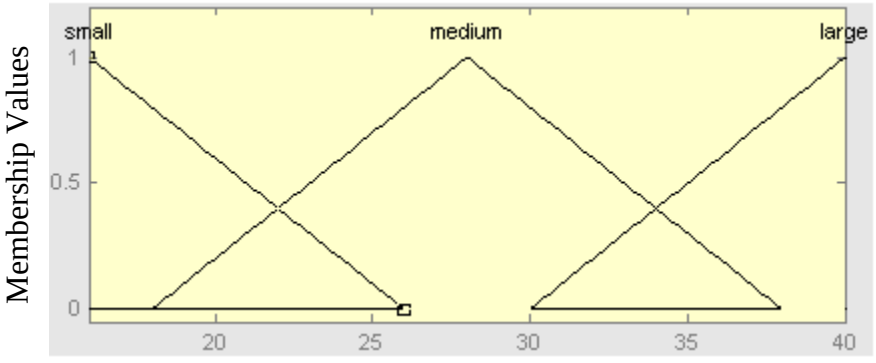

Figure 5.6: Membership functions for change in length

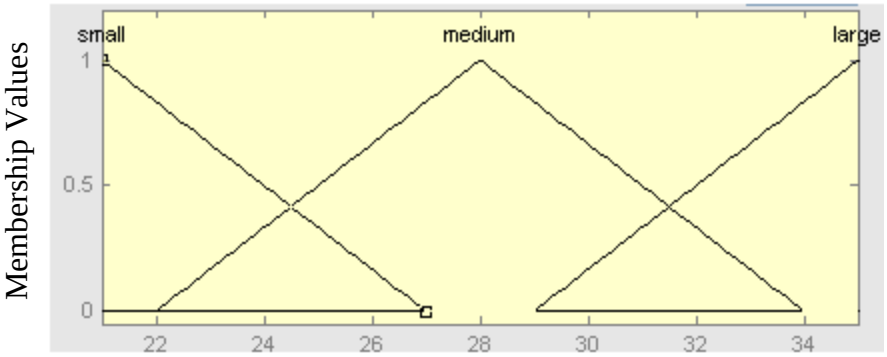

Figure 5.7: Membership functions for change in width

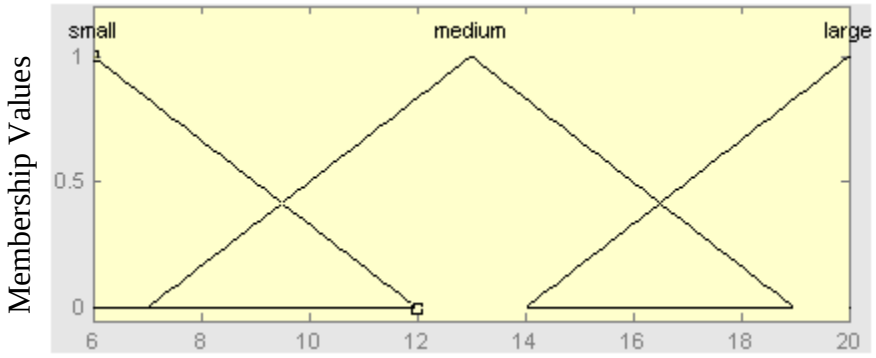

Figure 5.8: Membership functions for change in thickness

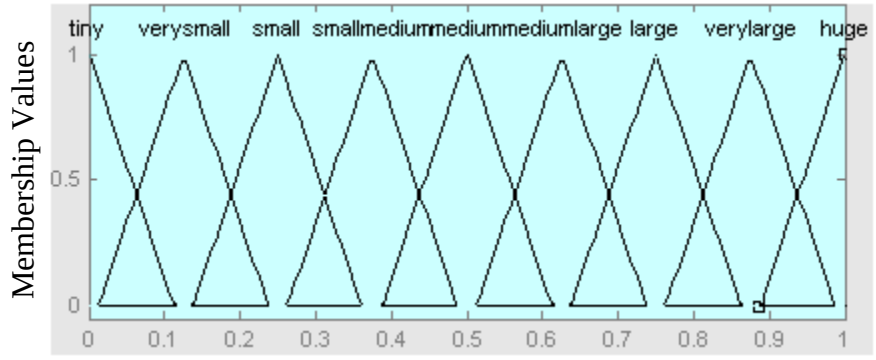

Figure 5.9: Membership functions for Multiresponse performance index

Twenty seven fuzzy rules (Table 5.7) are directly derived based on the fact that the larger the signal-to-noise ratio is, the better the performance characteristic. By taking the maximum-minimum compositional operation [54], the fuzzy reasoning of these rules yields a fuzzy output.

Table 5.7: Fuzzy rule table

Multiresponse-performance index	S/N ratio of ΔL		
	Small	Medium	Large
S/N ratio of ΔT	Small Medium Large	Small Medium Large	Small Medium Large
S/N ratio of ΔW			
Small	Tiny Very Small Small	Small Small Medium Medium	Small Medium Large
Medium	Very Small Medium Small Medium	Small Medium Medium Medium Large	Medium Large Very Large
Large	Small Medium Medium Large	Medium Medium Large Large	Medium Very Huge Large Large

Suppose x_1, x_2, x_3 are the three input values of the fuzzy logic unit, the membership function of the output of fuzzy reasoning can be expressed as:

$$\mu_D(y) = (\mu_{A_1}(x_1) \wedge \mu_{B_1}(x_2) \wedge \mu_{C_1}(x_3) \wedge \mu_{D_1}(y) \\ \vee \ldots\ldots\ldots (\mu_{A_n}(x_1) \wedge \mu_{B_n}(x_2) \wedge \mu_{C_n}(x_3) \wedge \mu_{D_n}(y)) \qquad (10)$$

where $\bigvee$ is the minimum operation and $\bigwedge$ is the maximum operation.

Finally, the defuzzifier transforms the fuzzy inference output $\mu_D(y)$ into a non-fuzzy value, which is known as multiresponse performance index by using Eq. (8). In this study, the rule base implementation in fuzzy logic toolbox in MATLAB was represented in Figure 5.10.

Based on the above discussion, the larger the multiresponse performance index is, the smaller the variance of performance characteristics around the desired value. Table 5.8 shows the

experimental results for the multiresponse performance index using the experimental layout (Table 3.2).

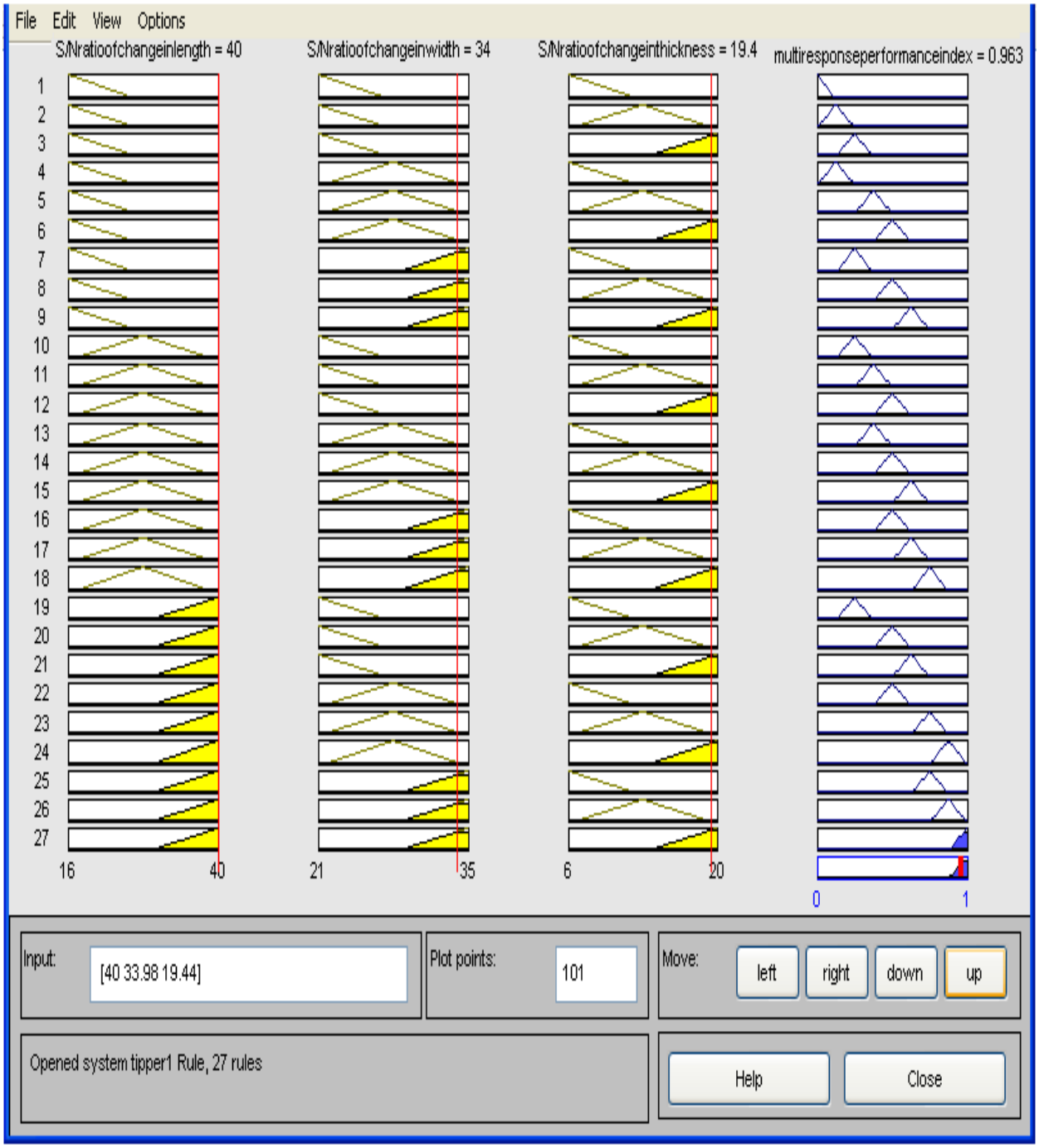

Figure 5.10: Creating rule base for fuzzy system by fuzzy logic tool box of Matlab

Table 5.8: Results for the Multiresponse performance index

Experiment Number	Multiresponse performance index
1	0.549
2	0.473
3	0.360
4	0.521
5	0.364
6	0.500
7	0.645
8	0.303
9	0.346
10	0.963
11	0.498
12	0.446
13	0.505
14	0.406
15	0.438
16	0.572
17	0.358
18	0.566
19	0.564
20	0.407
21	0.307
22	0.556
23	0.442
24	0.446
25	0.669
26	0.433
27	0.563

Main factor plot for multiresponse performance index (Figure 5.11) gives the optimum factor level as A_2, B_1, C_1, D_2, E_3. Thus, it is evident from Figure 5.11 that the factor combination of A2, B_1, C_1, D_2, and E_3 results in minimum change in dimensions of FDM built part. ANOVA for multiresponse performance index is shown in Table 5.9.

Results of the analysis of variance for MRPI indicate that A, B, C, E and B×C, B×D, B×E are the significant factors and interactions for affecting the multiple performance characteristics, where part orientation is the most significant. In addition, the change of raster width (D) in the range given by Table 3.1 and interaction A×B have insignificant effect on the defined multiresponse

performance index. As far as minimization of change in dimension is concerned, factors A, B, C, and E have significant effects while factor D has the least effect. Therefore, based on the above discussion, the optimal combination of FDM process parameters are the layer thickness at level 2, the orientation at level 1, the raster angle at level 1, the raster width at level 2, and the air gap at level 3.

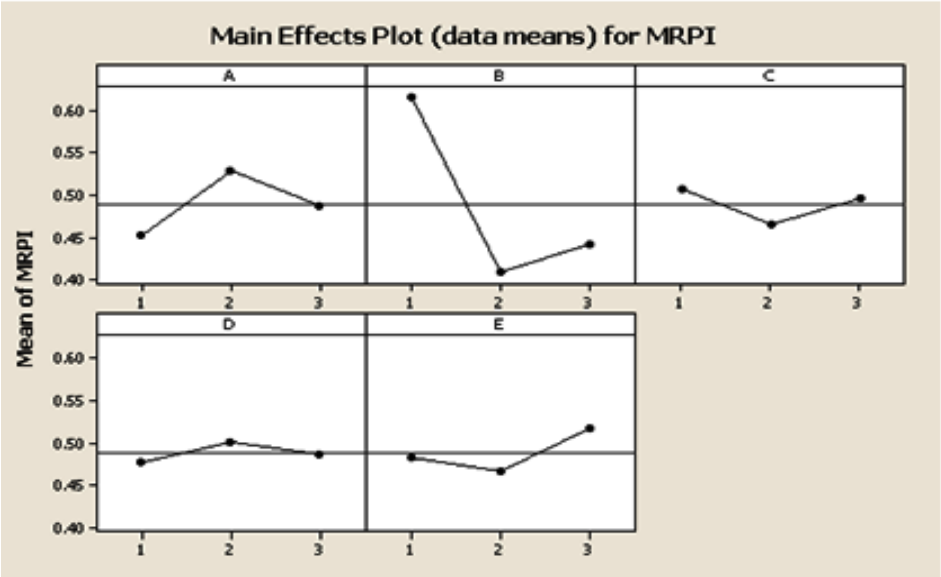

Figure 5.11: Main factor effect plot for multiresponse performance index

Table 5.9: ANOVA for Multiresponse performance index

Source	DOF	SS	MS	F	%P
A	2	0.0266	0.0133	8.87	5.56
B	2	0.2227	0.1114	74.27	46.59
C	2	0.0089	0.0045	3	1.90
D*		0.0026	0.0013	0.86	0.56
E	2	0.0117	0.0059	3.93	2.45
A×B*		0.0066	0.0016	1.06	1.38
B×C	4	0.0697	0.0174	11.6	14.58
B×D	4	0.0807	0.0202	13.47	16.88
B×E	4	0.0483	0.0121	8.07	10.10
Error	6	0.0092	0.0015		
Total	26	0.478			100

* Pooled

The predicted signal-to-noise ratio (η_{pre}) of a response can be calculated as:

$$\eta_{pre} = \eta_m + (\overline{A_i} - \eta_m) + (\overline{B_j} - \eta_m) + (\overline{C_k} - \eta_m) + (\overline{D_l} - \eta_m) + (\overline{E_n} - \eta_m) + [(\overline{A_i B_j} - \eta_m) - (\overline{A_i} - \eta_m) - (\overline{B_j} - \eta_m)] + [(\overline{B_j C_k} - \eta_m) - (\overline{B_j} - \eta_m) - (\overline{C_k} - \eta_m)] + [(\overline{B_j D_l} - \eta_m) - (\overline{B_j} - \eta_m) - (\overline{D_l} - \eta_m)] + [(\overline{B_j E_n} - \eta_m) - (\overline{B_j} - \eta_m) - (\overline{E_n} - \eta_m)] \quad (11)$$

where η_m is the total mean of the multiresponse performance index , $\overline{A_i}, \overline{B_j}, \overline{C_k}, \overline{D_l}, \overline{E_n}$ are the mean of multiresponse performance index for factors A, B, C, D, E at respective level i, j, k, l, n (i, j, k, l, n = 1, 2, 3), respectively. Factors and interactions which are insignificant will be omitted from Eq. (11).

Based on Eq. (11), the estimated multiresponse performance index using the FDM process parameters can then be obtained.

Two predictive models- one based on Taguchi and the other one using ANN have been proposed for MRPI prediction are validated using simulation studies. The experiments conducted as per orthogonal array is used for prediction purpose. In Taguchi additive model, orthogonal array having significant factors and interactions is used for estimation of MRPI. Due to presence of non-linearity in FDM process prediction of MRPI is done using conjugate gradient back propagation ANN. ANN splits the data into training and testing sets and the studies were carried out by using MATLAB simulation environment. The network is trained with selected input parameters (Table 4.1) for seventy five percent of experimental data as shown in Figure 5.12. The comparison between the experimental result and the predicted result based on Taguchi and ANN of OA data is shown in Table 5.10.

From the Table 5.10 it can be observed that the proposed ANN model provides mean absolute percentage error of 0.15 and 3.16 for Taguchi's additive model from experimental data. It is clear from the study that the ANN system gives the better result than Taguchi's predictive result.

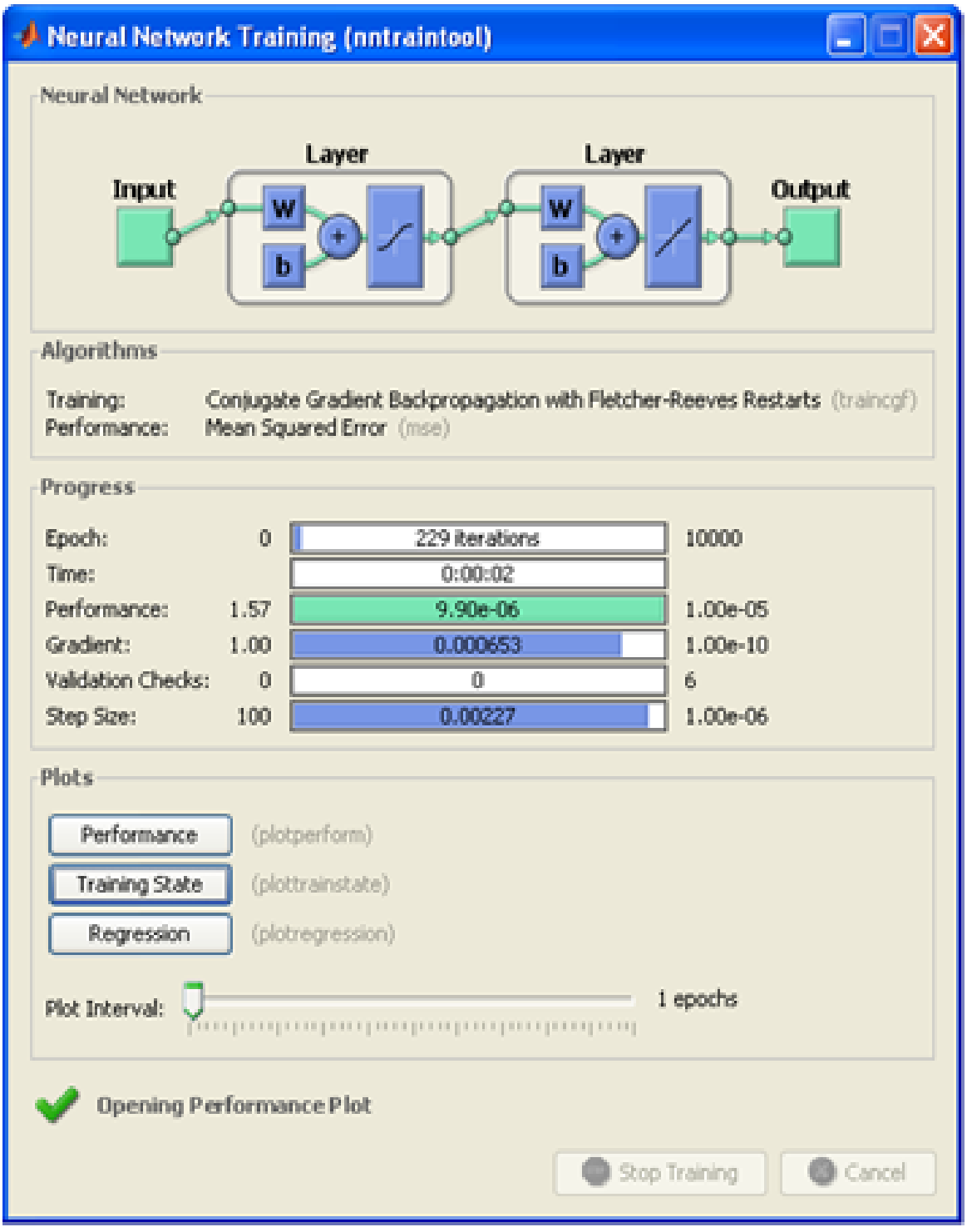

Figure 5.12: Artificial neural network training model

Table 5.10: Comparison of Experimental result, Taguchi and ANN predicted results of OA data

Exp.No.	MRPI using Mamdani model ($MRPI_{exp}$)	MRPI using Taguchi additive model ($MRPI_{th}$)	MRPI using ANN model ($MRPI_{ANN}$)
1	0.549	0.566	0.5503
2	0.473	0.451	0.4726
3	0.36	0.364	0.3604
4	0.521	0.514	0.5209
5	0.364	0.358	0.3636
6	0.5	0.513	0.4995
7	0.645	0.653	0.6454
8	0.303	0.306	0.3038
9	0.346	0.336	0.3457
10	0.963	0.925	0.9627
11	0.498	0.528	0.4982
12	0.446	0.455	0.4486
13	0.505	0.481	0.5047
14	0.406	0.445	0.4053
15	0.438	0.423	0.4358
16	0.572	0.558	0.5717
17	0.358	0.373	0.3586
18	0.566	0.566	0.5661
19	0.564	0.583	0.5639
20	0.407	0.398	0.4069
21	0.307	0.296	0.3069
22	0.556	0.584	0.5564
23	0.442	0.409	0.4393
24	0.446	0.449	0.4457
25	0.669	0.674	0.6691
26	0.433	0.416	0.4354
27	0.563	0.576	0.5628
Mean absolute percentage Error (%) with respect to MRPI exp		3.16	0.15

Regression results of $MRPI_{exp}$ Vs $MRPI_{ANN}$ for training and testing data sets are shown in Figures 5.13 and 5.14. From the Figure 5.14, it is observed that R^2 value for testing is found to be 0.972 and thus, the network is well trained. Based on convergence criterion (Table 4.1) employed in the network training, the training performance curve of conjugate gradient back propagation with Fletcher-Reeves update ANN model is shown in Figure 5.15. From the Figure 5.15, it is found that at 229 epochs mean square error or goal is achieved.

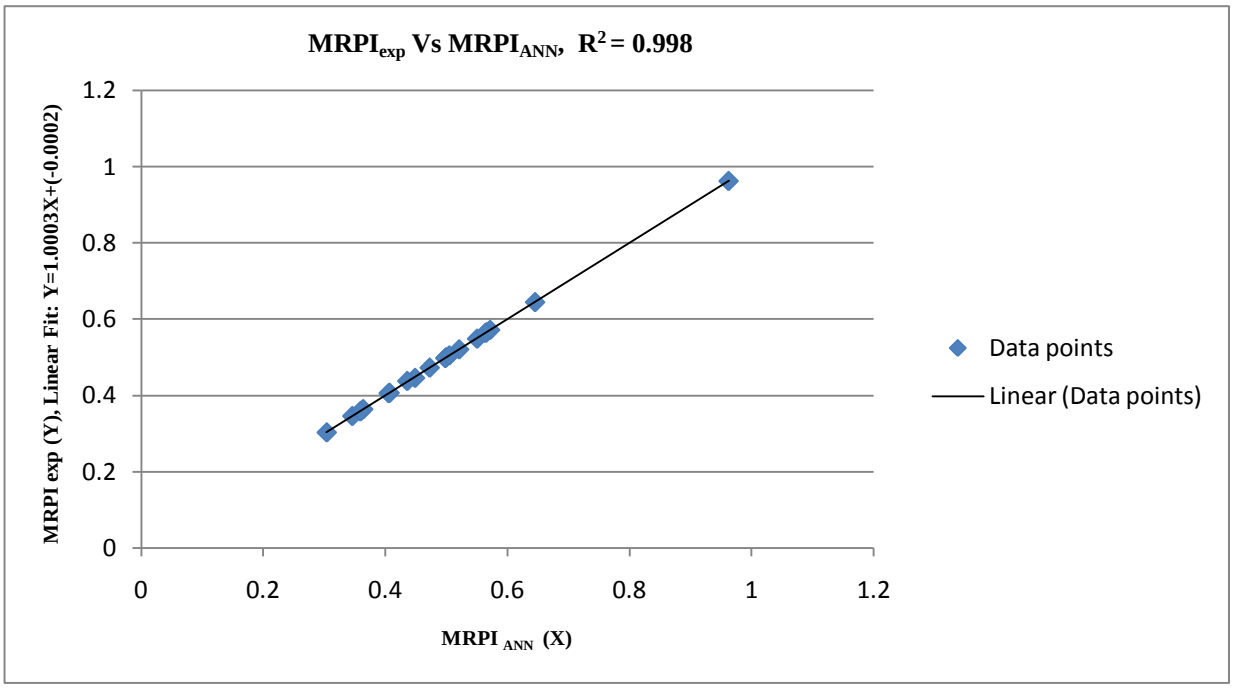

Figure 5.13: Regression plot of $MRPI_{exp}$ Vs $MRPI_{ANN}$ for training data set

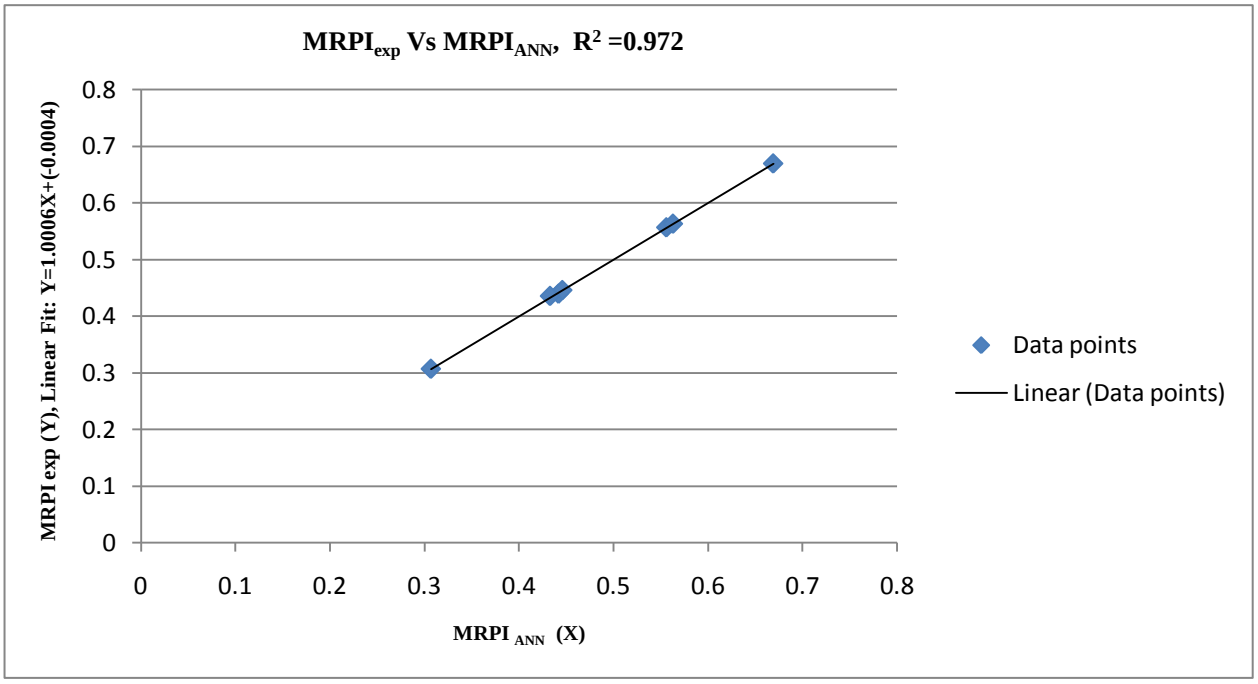

Figure 5.14: Regression plot of $MRPI_{exp}$ Vs $MRPI_{ANN}$ for testing data set

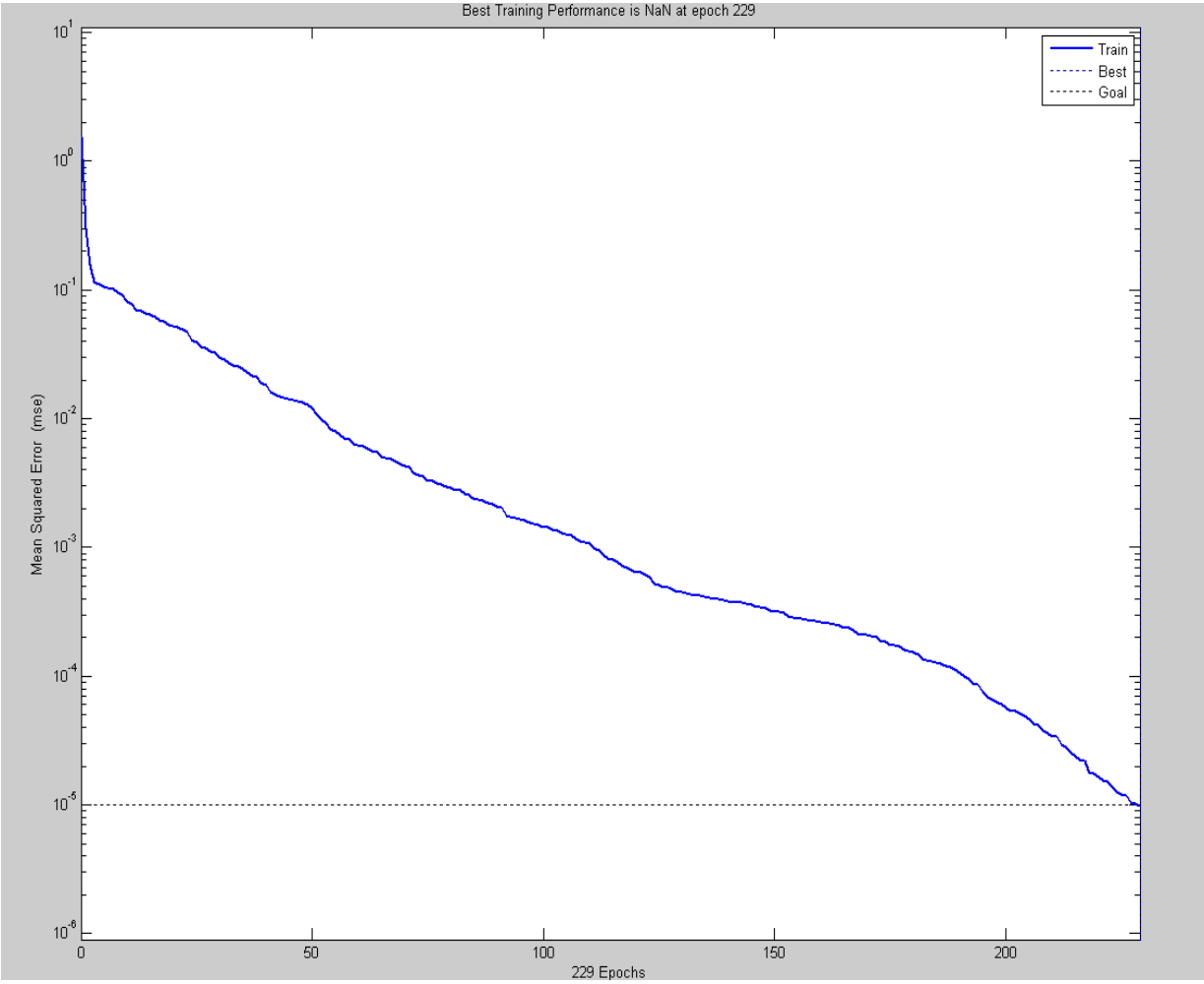

Figure 5.15: Training performance curve

The main advantage of the ANN model lies in the fact that it enables to predict the output beyond the experimental layout by simply inputting the parameters in a specified domain value if properly trained but Taguchi's additive model fails to do the same without having experimental data for which substantial amount of energy, time and materials are required. Hence, the proposed ANN model will be easily implemented in a hardware system as compared to Taguchi model. Further, the ANN model outperform Taguchi's predictive model because it is of additive in nature and hardly incorporates non-linearity which is a found in real life situations particularly in the study of dimensional accuracy of FDM built parts.

Since part orientation seems to influence to a great extent as compared to other factors, therefore selection of orientation is very important for obtaining accuracy in part dimensions and higher quality in dimensional accuracy of FDM processed part can be achieved with minimum part orientation. However, the relative importance of the different FDM process parameters for the multiple performance characteristics must still be known so that the optimal combination of the parameter levels can be determined more accurately.

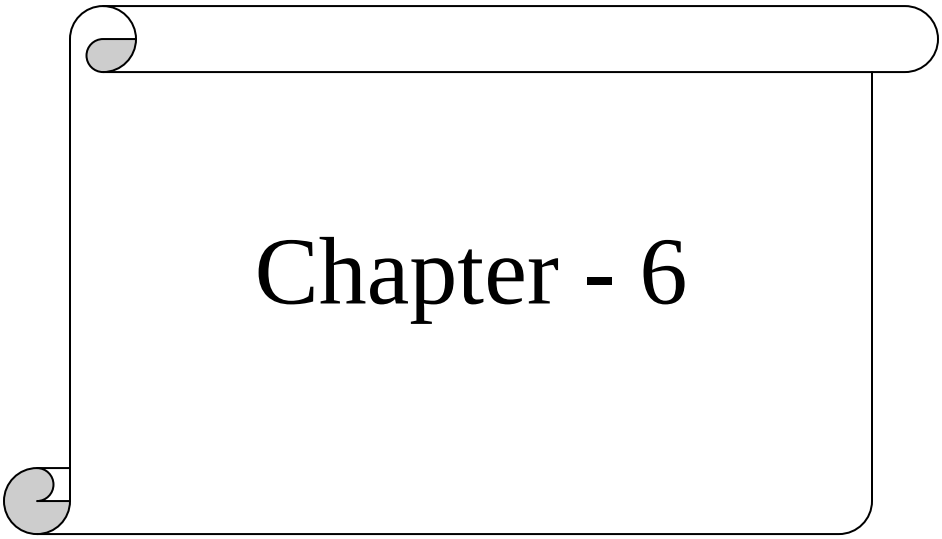
Chapter - 6

Chapter 6

CONFIRMATION TESTS

The confirmation experiment is performed by taking an arbitrary initial set of control parameter combination beyond the experimental layout. Once the optimal level of the process parameters is selected, based on Eq. (11) the multiresponse performance index using the optimal FDM parameter can be estimated. Factor D and interaction A×B has been intentionally omitted for all the cases because they have insignificant effect on the multiple performance characteristics. The calculated predicted value is compared with the experimental result and the error associated is determined. The initial FDM parameters were taken as A_1, B_1, C_2, D_2, E_1 and at this setting experiment is conducted three times. Readings of length, width and thickness are taken per sample and mean is taken as the representative value for each of these dimensions. The values of ΔL, ΔW and ΔT are found to be 0.0391 mm, 0.0768 mm and 0.1079 mm. Table 6.1 shows the results of the confirmation experiment using the optimal FDM parameters.

Table 6.1: Results of the confirmation experiment

	Initial FDM Parameters	Optimal FDM parameters	
		Prediction	Experiment
Level	$A_1B_1C_2\ D_2E_1$	$A_2B_1C_1D_2E_3$	$A_2B_1C_1D_2E_3$
ΔL (mm)	0.0391		0.0099
ΔW (mm)	0.0768		0.0200
ΔT (mm)	0.1079		0.1066
MRPI	0.509	0.925	0.963
		Improvement MRPI = 0.454	

As shown in Table 6.1, the ΔL is decreased from 0.0391 mm to 0.0099 mm, ΔW is decreased from 0.0768 mm to 0.0200 mm and the ΔT is decreased from 0.1079 mm to 0.1066 mm through this study. Percentage of error between experimental result and calculated predicted value is found to be 3.94 (absolute). Since the error is within the tolerance limit, therefore the Taguchi's model is considered to be capable of predicting MRPI to a reasonable accuracy.

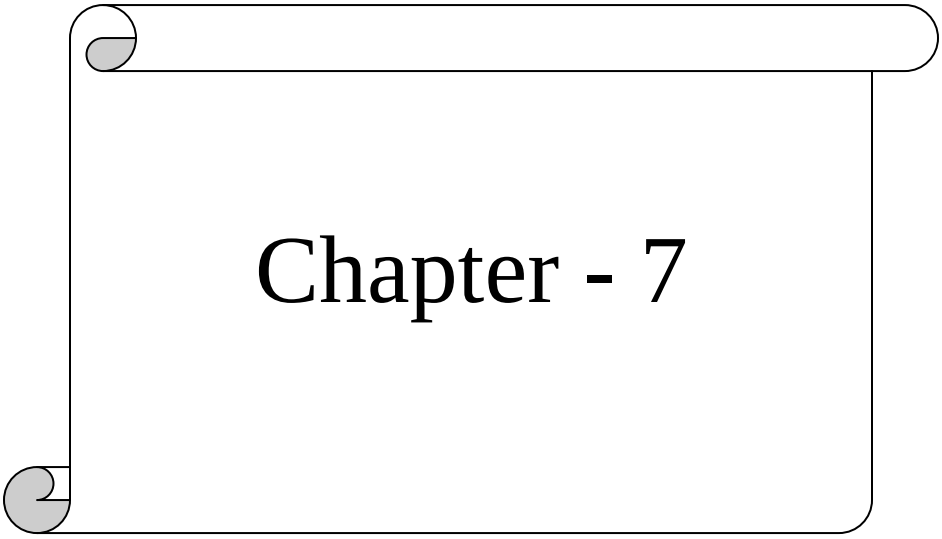
Chapter - 7

Chapter 7

CONCLUSIONS

In the present work, application of fuzzy logic reasoning using the Taguchi method for improvement of dimensional accuracy of FDM processed part is studied. The optimization of the process parameters for minimum change in length, width and thickness has been performed individually. But, it has been observed that a large number of conflicting factors independently or in interaction with others may influence the dimensional accuracy. Few of them have more influence in comparison to others. Therefore, instead of considering factor settings in an arbitrary manner, it is proposed that fabrication process must be based on optimum settings obtained through a structured methodology. It is desirable to fabricate the parts in such a manner that all the dimensions should show minimum deviation from desired value simultaneously, at the common factor level setting. As a result, fuzzy logic method is adopted and the performance characteristics such as change in length, width and thickness can be simultaneously considered and improved through this approach. After carrying out experimental investigations for selecting optimum combination of process parameters on FDM part dimensions, the following conclusions can be drawn:

(i) The optimal levels of process parameters for minimum change in length, width and thickness are: Layer thickness of 0.178mm, orientation of 0^0, raster angle of 0^0, raster width of 0.4564mm and air gap of 0.008mm.

(ii) The contribution of part orientation is largest in comparison with other process parameters for controlling the change in dimensions of FDM built part.

(iii) The confirmation test results in improvement of multiresponse performance index (Improvement MRPI=0.454) using the optimal FDM parameters over initial FDM parameters and proposed equation for predicting multiresponse performance index is valid.

Further, two predictive models- one based on Taguchi approach and the other on ANN approach are proposed. It is demonstrated that these models well reflect the effects of various factors on accuracy in dimensions and their predictive results are consistent with experimental observations. The mean absolute error percentage between experimental and Taguchi model is found to be 3.16 whereas ANN model results in 0.15.

The present study has observed that part orientation is the main controlling factor for achieving better dimensional accuracy.

Scope for Future work

In future, this study will open up further scope of optimization of FDM characteristics considering larger number of process parameters and their influences on intricate geometry parts for achieving better quality with faster rate.

References

[1] Chua, C. K., Feng, C., Lee, C. W., and Ang, G.Q. (2005), "Rapid investment casting: direct and indirect approaches via model maker II.", International Journal of Advanced Manufacturing Technology, 25, 11-25.

[2] Zhong, W. H. (1999), "Rapid prototyping manufacturing technology and its development.", Aerospace Materials and Technology, 29(3), 23-26

[3] Wiedemann, B. and Jantzen, H. A. (1999), "Strategies and applications for rapid product and process development in Daimler-Benz AG.", Computers in Industries, 39(1), 11-25.

[4] Upcraft, S. and Fletcher, R. (2003), "The rapid prototyping technologies.", Rapid Prototyping Journal, 23(4), 318-30.

[5] Mansour, S., Hauge, R. (2003), "Impact of rapid manufacturing on design for manufacturing for injection moulding.", Proceedings of the Institution of Mechanical Engineers: Journal of Engineering Manufacture, Part B, 217(4), 453-461.

[6] Huang, Y. M. and Hsiang, Y. L. (2006), "Path planning effect on the accuracy of rapid prototyping system.", International Journal of Advanced Manufacturing Technology, 30, 233-246.

[7] Bernarand, A. and Fischer, A. (2002), "New trends in rapid product development.", CIRP annals-Manufacturing Technology, 51(2), 635-652.

[8] Zhong, W. H., Li, F., Zhang, Z. G., Song, L. and Li, Z. (2001), "Short fiber reinforced composites for fused deposition modeling.", Journal of Materials Science and Engineering A, 301, 125-130.

[9] Pham, D. T. and Dimov, S. S. (2001), Rapid manufacturing, Springer-Verlag, 360, Page 6.

[10] Wohlers Report (2009), "State of the Industry Annual Worldwide Progress Report on Additive Manufacturing.", Wohlers Associates.

[11] Levy, G. N., Schindel, R., Kruth, J. P. and Leuven, K. U. (2003), "Rapid manufacturing and rapid tooling with layer manufacturing (LM) technologies – State of the art and future perspectives.", CIRP annals-Manufacturing Technology, 52(2), 589-609.

[12] Pilipovic, A., Raos, P. and Sercer, M. (2009), "Experimental analysis of properties of materials for rapid prototyping.", International Journal of Advanced Manufacturing Technology, 40, 105–115.

[13] Rosochowski, A., Matuszak, A. (2000), “Rapid tooling – the state of art.”, Journal of Materials Processing Technology, 106, 191–198.

[14] Hopkinson, N., Hagur, R. J. M. and Dickens, P. H. (2006), “Rapid manufacturing: an industrial revolution for the digital age.”, England: John Wiley & Sons Inc.

[15] Chockalingama, K., Jawahara, N., Chandrasekarb, U. and Ramanathana, K. N. (2008), “Establishment of process model for part strength in stereolithography.”, Journal of Materials Processing Technology, 208, 348-365.

[16] Ross, P. J. (1998), “Taguchi techniques for quality engineering.”, McGraw Hill, New York.

[17] Bendell, A., Disney, J. and Pridmore, A. (1989), “Taguchi methods: Applications in world industry”, IFS publications, UK.

[18] Sood, A. K., Ohdar, R. K. and Mahapatra, S. S. (2009), “Improving dimensional accuracy of fused deposition modeling processed part using grey Taguchi method.”, Materials and Design, 30, 4243-4252.

[19] Elsayed, E. A. and Chen, A. (1993), “Optimal levels of process parameters for products with multiple characteristics.”, International Journal of Production Research, 31(5), 1117-1132.

[20] Phadke, M. S. (1989), “Quality engineering using robust design.”, Prentice Hall, Englewood Cliffs, New Jersey.

[21] Vasudevarao, B., Natarajan, D. P., Razdan, A. and Mark, H. (2000), “Sensitivity of RP surface finish to process parameter variation.”, In: Solid free form fabrication proceedings, The University of Texas, Austin, 252-258.

[22] Es Said, Os., Foyos, J., Noorani, R., Mandelson, M., Marloth, R. and Pregger, B.A. (2000), “Effect of layer orientation on mechanical properties of rapid prototyped samples.”, Materials and Manufacturing Process, 15(1), 107-122.

[23] Khan, Z. A., Lee, B. H. and Abdullah, J. (2005), “Optimization of rapid prototyping parameters for production of flexible ABS object.”, Journal of Materials Processing Technology, 169, 54-61.

[24] Lee, C. S., Kim, S. G., Kim, H. J. and Ahn, S. H. (2007), "Measurement of anisotropic compressive strength of rapid prototyping parts.", Journal of Materials Processing Technology, 187–188, 627-630.

[25] Anitha, R., Arunachalam, S. and Radhakrishnan, P. (2001), "Critical parameters influencing the quality of prototypes in fused deposition modeling.", Journal of Materials Processing Technology, 118, 385-388.

[26] Ming, W. T., Tong, X. J. and Ye, J. (2007), "A model research for prototype warp deformation in the FDM process.", International Journal of Advanced Manufacturing Technology, 33(11–12), 1087-1096.

[27] Chou, K. and Zhang, Y. (2008), "A parametric study of part distortion in fused deposition modeling using three dimensional element analysis.", Proceedings of the Institution of Mechanical Engineers: Journal of Engineering Manufacture, 222(B), 959-967.

[28] Pandey, P. M. and Ragunath, N. (2007), "Improving accuracy through shrinkage modeling by using Taguchi method in selective laser sintering.", International Journal of Machine Tools and Manufacture, 47, 985-995.

[29] Zhou, J. G., Herscovici, D. and Chen, C. C. (2000), "Parametric process optimization to improve the accuracy of rapid prototyped stereolithography parts.", International Journal of Machine Tools and Manufacture, 40, 363-379.

[30] Campanelli, S. L., Cardano, G., Giannoccaro, R., Ludovic, A. D. and Bohez, E. L. J. (2007), "Statistical analysis of stereolithographic process to improve the accuracy.", Computer Aided Design, 39(1), 80-86.

[31] Ahn, S. H., Montero, M., Odell, D., Roundy, S. and Wright, P. K. (2002), "Anisotropic material properties of fused deposition modeling ABS.", Rapid Prototyping Journal, 8(4), 248-257.

[32] Venkata, R. N., Pandey, P. M. and Dhande, S. G. (2007), "Part deposition orientation studies in layered manufacturing.", Journal of Materials Processing Technology, 185, 125-131.

[33] Byun, H. S. and Lee, K. H. (2006). "Determination of the optimal build direction for different rapid prototyping processes using multi-criterion decision making.", Robot Computer Integrating Manufacturing, 22, 69-80.

[34] Bellehumeur, C. T., Gu, P., Sun, Q. and Rizvi, G. M. (2008), "Effect of processing conditions on the bonding quality of FDM polymer filaments.", Rapid Prototyping Journal, 14(2), 72-80.

[35] Pandey, P. M., Jain, P. K. and Rao, P. V. M. (2009), "Effect of delay time on part strength in selective laser Sintering.", International Journal of Advanced Manufacturing Technology, 43, 117-126.

[36] Too, M. H., Leong, K. F., Chua, C. K., Du, Z. H., Yang, S. F., Cheah , C. M. and Ho, S. L. (2002), "Investigation of 3D Non Random Porous Structures by Fused Deposition Modeling.", The International Journal of Advance Manufacturing Technology, 19, 217-223.

[37] lppolito, R. L., luliano, P., Torino, D. and Gatto, A. (1995), "Benchmarking of Rapid Prototyping Techniques in Terms of Dimensional Accuracy and Surface Finish.", CIRP Annals-Manufacturing Technology, 44 (1), 157-160.

[38] Marissen, R., Schudy, D., Kemp, A.V.J.M., Coolen, S.M.H., Duijzings, W.G., Van Der Pol, A. and Van Gulick , A.J. (2001), "The effect of material defects on the fatigue behaviour and the fracture strain of ABS.", Journal of Polymer Science, 36, 4167-4180.

[39] Jar, P.Y.B., Konoshi, K. and Shinmura, T. (2002), "Characterization of toughness variation due to intrinsic defects in high-thermal-resistant poly(acrylonitrile-butadiene-styrene) (ABS).", Journal of Polymer Science, 37, 4521-4528.

[40] Stratasys, FDM Vantage user guide version 1.1. 2004. <www.stratasys.com>.

[41] Stuart, P. G. (1993), "Taguchi methods: a hand on approach.", New York: Addison Wesley publishing company.

[42] Noorani, R. (2005), "Rapid prototyping – principles and application.", New Jersey: John Wiley & Sons Inc.

[43] Zadeh, L. A. (1965), "Fuzzy Sets.", Information and Control, 8, 338-353.

[44] Zadeh, L. A. (1976), "A Fuzzy-algorithm Approach to the Definition of Complex or Imprecise concept.", International Journal of Man-Machine Studies, 8, 249-291.

[45] Mendel, J. M. (1995), "Fuzzy Logic Systems for Engineering: A Tutorial.", IEEE Proceedings, 83, 345-377.

[46] Cox, E. A. (1992), "Fuzzy Fundamentals.", IEEE Spectrum, 29, 58-61.

[47] Mamdani, E. H. and Assilia, S. (1975), "An Experiment in Linguistic Synthesis with a Fuzzy Logic Controller.", International Journal of Man-Machine Studies, 7, 1-13.

[48] Jang, J. S. R., Sun, C. T. and Mizutan, E. (2005), "Neuro-Fuzzy and Soft Computing.", Prentice Hall of India Private Limited, New Delhi.

[49] Rajasekaran, S. and Pai, G.A.Vijayalakshmi. (2003), "Neural Networks, Fuzzy Logic and Genetic Algorithms - Synthesis and Applications.", Prentice Hall of India Pvt. Ltd., New Delhi.

[50] Hagen, M. T., Demuth, H. B. and Beale, M. H. (1996), Neural Network design, PWS publishing, Boston.

[51] Nickel, A. H., Barnett, D. M. and Prinz, F. B. (2001), "Thermal stresses and deposition patterns in layered manufacturing.", Materials Science and Engineering, A317, 59-64.

[52] Liao, Y. S. and Chiu, Y. Y. (2001), "A new slicing procedure for rapid prototyping systems.", International Journal of Advanced Manufacturing Technology, 18, 579-585.

[53] Pandey, P. M., Venkata, R. N. and Dhande, S. G. (2003), "Slicing procedures in layered manufacturing a review.", Rapid Prototyping Journal, 9(5), 274-288.

[54] Zimmerman, H. J. (1985), "Fuzzy set theory and its applications.", Kluwer, London.